

Regional significance of historical trends and step changes in Australian streamflow

Gnanathikkam Emmanuel Amirthanathan¹, Mohammed Abdul Bari², Fitsum Markos Woldemeskel¹, Narendra Kumar Tuteja^{3*}, Paul Martinus Feikema¹

5 ¹Bureau of Meteorology, Melbourne, Australia.

²Bureau of Meteorology, Perth, Australia.

³Bureau of Meteorology, Canberra, Australia.

*Current address WaterNSW, Sydney

10 *Correspondence to:* Mohammed Bari (mohammed.bari@bom.gov.au)

Abstract. The [Hydrologic Reference Stations](#) is a network of 467 high quality streamflow gauging stations across Australia, developed and maintained by Bureau of Meteorology, as part of ongoing responsibility under the [Water Act 2007](#). The main objectives of the service are to observe and detect climate-driven changes in observed streamflow and to provide a quality controlled dataset for research. We investigate trends and step changes in streamflow across Australia in data from all 467 streamflow gauging stations. Data from 30 to 69 years duration ending in February 2019 was examined. We analysed data in terms of water year totals and for the four seasons. The commencement of water year varies across the country – mainly from February–March in the south to September–October in the north. We summarised our findings for each of the 12 Drainage Divisions defined by [Australian Geospatial Fabric \(Geofabric\)](#), and continental Australia as a whole. We used statistical tests to detect and analyse linear and step changes in seasonal and annual streamflow. Monotonic trends were detected by Mann-Kendall – Variance Correction Approach (MK3), Block Bootstrap Approach (MK3bs) and Long Term Persistence (Mk4) tests. The Nonparametric Pettitt test was used for step change detection and identification. Regional significance of these changes at the drainage division scale was analysed and synthesised using the Walker test. The Murray Darling Basin, with Australia’s largest river system, showed statistically significant decreasing trends for the region in annual total and all four seasons. Drainage Divisions in New South Wales, Victoria and Tasmania showed significant annual and seasonal decreasing trends. Similar results were found in south-west Western Australia, South Australia and north-east Queensland. There was no significant spatial pattern observed in Central and mid-west Australia, one possibility being the sparse density of streamflow stations and or length of data. Only the Timor Sea drainage division in northern Australia showed increasing trends and step changes in annual and seasonal streamflow and were regionally significant. Most of the step changes occurred during 1970–99. In the south-eastern part of Australia, majority of the step changes occurred in the 1990s, before the onset of the millennium drought. Long term monotonic trends in observed streamflow and its regional significance are consistent with observed changes in climate experienced across Australia. Findings from this study will assist water managers for long term infrastructure planning and management of water resources under climate variability and change across Australia.

1 Introduction

Australia is the driest inhabited continent on Earth, receiving only 450mm/yr of rainfall on average (CSIRO and BOM, 2020). Rainfall amounts vary significantly across the country, with approximately 70 percent of the landmass being arid or semi-arid receiving less than 350mm/yr (BOM, 2022). The distribution and amount of rainfall across the country has influenced patterns of human settlement for more than 60,000 years (Williams, 2013). The continent also has unique topographic and geologic features. The central region is mostly arid or semi-arid, south-east and south-west corners having temperate, and the north having tropical climate (Stern et al., 2000). The east and south-east coastal regions have mountain ranges. Rainfall is higher and more reliable in coastal regions, except mid-west coastal regions of Western Australia. Elevation is another factor that has an important influence on rainfall, with mountainous areas such as northeast Queensland, southeast Australia and western Tasmania receiving higher rainfall (Holper, 2011). Rainfall is highly variable in both space and time compared to other continents. Together with unique topographic and geological features and distribution of rainfall result in the greatest interannual variability in streamflow (Nicholls et al., 1997; Poff et al., 2006), floods and droughts.

The ‘Millennium Drought’ between 1997 and 2009 is described as the worst drought on record for southeast Australia (Van Dijk et al., 2013). During 2001-2009, southeast Australia suffered the driest period since 1900 – the longest uninterrupted series of years with below median rainfall (Bureau of Meteorology data; <http://www.bom.gov.au/cgi-bin/climate/change/timeseries.cgi>). Discharge of the River Murray System during this period were half the previous recorded minimum. As a response to the widespread social, financial and environmental impacts of drought, the federal government passed the Water Act 2007 (<https://www.legislation.gov.au/Details/C2017C00151>) legislation through the parliament heralding the implementation of the water security plan for Australia. One of the important roles in realising the water security plan is enhancing our understanding of Australia’s water resources. The Hydrologic Reference Station service (<http://www.bom.gov.au/water/hrs/index.shtml>) was developed to provide greater insight of climate-driven changes in streamflow across Australia. Similar services exist in Canada, United States, Europe (Bradford and Marsh, 2003; Brimley et al., 1999; Coxon et al., 2020; Falcone et al., 2010; Lins, 2012; Whitfield et al., 2012) and in other areas across the globe (Alfieri et al., 2020). In Canada, spatial and temporal trends in streamflow and other associated hydroclimatic variables show increasing and decreasing patterns in northern and mid-latitude catchments, respectively (Bawden et al., 2015; O’Neil et al., 2017). In the continental United States, streamflow analyses from 1940 to 2009 for 967 gauging stations, show overall decreasing trends, including higher annual maxima, and lower annual minima (Rice et al., 2015). Similar results were also found by Asadieh, et al. (2016) over the 1971-2001 period in the United States and other continents across the world. When comparing trends in minimally altered or regulated catchments in the United States, Hodgkins, et al. (2020) found there were larger changes in median streamflow compared to changes in annual 1-day high or 7-day low flows. Shifts in flood peaks and streamflow timing were found to be consistent with changes in rainfall, in both natural and managed catchments (Ficklin et al., 2018). In Finland, trend analysis revealed no changes in mean annual flow overall, but some changes in seasonal distribution of streamflow (Korhonen and Kuusisto, 2010). In south-east Asia and Africa, analyses of observed streamflow mostly show downward trends. In the Senegal river basin analysis of annual streamflow showed decreasing trends (Diop et al., 2018), while dry season flows increased by 6% at the Black Volta basin in West Africa over the period 2000 to 2013 (Akpoti et al., 2016). Decreasing trends were also

75 found in streamflow extremes across China (Li et al., 2020), and in streamflow in Huaihe River Basin, China (Pan et al., 2018). Similar trends were also evident in annual streamflow in West Borneo, Indonesia (Herawati et al., 2015).

80 Global-scale investigation of trends in annual maximum streamflow reveal decreasing trends tend to occur in Asia, Australia, the Mediterranean, the western and north-eastern United States, and northern Brazil, increasing trends appear mostly in central North America, southern Brazil and the northern part of western Europe (Do et al., 2017). Rainfall is one potential driver of these changes. Analyses of streamflow trends, using data from more than 30,000 gauges across the world, Gudmundsson, et al. (2019) found that where trends are present in a region, direction of the trend is often consistent across all trend analyses indicators including high, average and low flows for that specific region. Analyses of floods and extreme streamflow events across the world show little to suggest 85 that increases in heavy rainfall events at higher temperatures result in similar increases in streamflow (Wasko and Sharma, 2017). However, shifts in timing of flood peaks and changes in streamflow timing were found to be consistent with rainfall change and in a similar direction (Wasko et al., 2020).

90 Australian streams showed the greatest influence by interannual variability in flow (Poff et al., 2006). Chiew and McMahon (1993) examined annual streamflow series of 30 unregulated Australian catchments to detect trends or changes in the means. They concluded that any changes were directly related to interannual variability rather than any changes in climate. Analysis of trends in Australian flood data from 491 stations (Ishak et al., 2010) indicated that about 30% showed trends in annual maximum flood, with downward and upward trends in southern and northern part of Australia, respectively. Analyses of 780 unregulated catchments (Gu et al., 2020) reveal similar 95 geographical distribution in trends. Other studies have investigated trends in selected streamflow components in particular regions – in the southwest of Western Australia (Durrant and Byleveld, 2009; Petrone et al., 2010) and in southeast Victoria (Tran and Ng, 2009). In Victoria and the Australian Alps, assessment and reconstruction of 100 catchment variability and trends in streamflow showed a decline during the period 1977–2012 (Fiddes and Timbal, 2016). Similar spatial pattern in streamflow reduction also occurred during the Millennium Drought between 1997-2009. Johnson et al (2016) reviewed historical trends and variability in flood events across Australia and concluded that the link between trends in flood events and rainfall cannot be made due to the influence of climate 105 processes such as temperature and evapotranspiration over different spatial and temporal scales. Similar results were also found by Wasko and Nathan (2019) and Sharma et al. (2018) – that changes in rainfall and soil moisture did not always explain trends in flooding.

110 The studies above undertook trend analysis of Australian rivers with limited spatial or temporal coverage of streamflow data. This study undertakes a systematic appraisal of changes and trends in observed streamflow records in a large number of catchments across the country which are largely unaffected by human influence. Zhang et al. (2016) undertook the first comprehensive study employing the Hydrologic Reference Stations and analysed data until 2014 from 222 stations across Australia. That study investigated many components of streamflow including annual total, high and low flows, seasonal totals and baseflow components were analysed and presented in the website <http://www.bom.gov.au/water/hrs>. The above study considered only the streamflow variables that are random and did not consider the effect of the autocorrelation structure and long-term persistence on the trend of streamflow variables. The Hydrologic Reference Stations service is now updated and contains information for 467 gauging stations and streamflow data to February 2019. In this study, we focus on monotonic

trends and step changes in annual and seasonal streamflow across different drainage divisions of Australia, and 115 its regional significance. Investigation of changes in other streamflow variables or driving forces of changes in rainfall patterns on these resulting trends in streamflow is out of scope of this study. Results from this study will benefit managers and researchers in sustainable water management and long-term planning in water allocation, agricultural planning, and hydropower.

2 Selection of gauging stations and data quality

120 2.1 Station selection guidelines

Guidelines for selection of the Hydrologic Reference Stations (HRS) were described in detail by Turner et al. 125 (2012). These include a minimum of 30 years of continuous data with less than 5% of missing data in unimpaired catchments. Details of station selection procedure is provided in the HRS website. In the recent update of the service, the Bureau of Meteorology implemented two additional criteria: (i) the percentage of flow volume included as infilled data and, (ii) the percentage of flow volume above the maximum gauged discharge. The thresholds for these two criteria were: (i) a maximum of 10% for flow volume of infilled data and, (ii) a restriction in extrapolated data to a maximum of 25%. Details of the station selection guidelines are presented in the [website](#). All of the 467 gauging stations that met these guidelines and were included in the updated service are included in this study.

130 2.2 Updated number of gauging stations

2.2.1 Gauging stations in 2020 update

Of the existing 222 gauging stations in the network prior to the service (Zhang et al., 2016), 12 are now 135 decommissioned by the data providing agencies, including 5 from Northern Territory, 2 from Victoria, 2 from Western Australia, 1 from New South Wales and 2 from South Australia. The revised and updated selection guidelines were applied to the remaining 210 gauging stations, and 179 of these stations passed the new guidelines. More information about rating curves of 43 existing stations are now available which suggests that these stations do not pass selection criteria. Therefore these 43 stations were removed from HRS service in 2020 (Table 1).

2.2.2 New stations included in the service

Australia's instrumental record is relatively sparse before 1940, and few locations have continuous rainfall 140 measurement before 1900. At present, there are approximately 4,800 streamflow gauging stations across Australia. Many of these stations previously had insufficient data in Bureau's system to be considered for the HRS service. Over recent years, more data has become available, and a set of 780 stations identified by Zhang et al. (2013) were 145 selected for further investigation. These 780 unregulated, unimpaired catchments are widely spread across Australia (Fig. 1), and have undergone strict quality assurance and quality control, including quality code checking for daily streamflow records (Zhang et al., 2013). The total number of streamflow gauging stations that met the new guidelines and are now included in the service is 467, which is an increase from 222 stations (Table 1).

2.2.3 Reference period, quality control and catchment description

The HRS was updated with streamflow data ending in February 2019. This month was chosen to capture the 2018

water year for all stations. Commencement of recording of streamflow data varies across the country. The longest

150 record begins from 1950s and the shortest one from 1980s. Figure 1 shows the location of stations and duration

of record, and includes the 8 decommissioned stations. Data recorded at stations prior to 1950 was excluded from

analysis, as the missing data were more than 5% before this time in most of the cases. Stations with longest records

are generally those in the high-value water resource catchments and populated areas along the coastal regions.

Upstream catchment area also varied across the country (from 4.5 to 232,846 km²) and in different hydroclimatic

155 regions (Table 2). Most of the catchment area ranged from 50 km² to 10,000 km² (Table 2). The number of stations

distributed across different drainage divisions vary substantially – Murray Darling division having the largest

number of stations while the South-Western Plateau has no stations at all. Drainage divisions are defined according

to [Australian Hydrological Geospatial Fabric \(Geofabric\) \(Atkinson et al., 2008\)](#). In the previous update of the

HRS service (Zhang et al., 2016), there were no stations in Pilbara-Gascoyne and North Western Plateau divisions.

160 In the current version there are 10 and 2 stations, respectively (Fig. 1, Table 2).

The continental Australia has a wide range of climate zones as defined by Köppen Climate Classification (Stern

et al., 2000) – including tropical region in the north, temperate regions in the south, grassland and desert in the

vast interior (Fig. 1). Water year is defined in accordance with the Hydrologic Reference Station [Glossary](#)

[\(<http://www.bom.gov.au/water/hrs/glossary.shtml>\)](http://www.bom.gov.au/water/hrs/glossary.shtml). It varies across the country - begins February-March in the

165 south and September-October in the north (Table 2). Annual average rainfall for each of the divisions vary from

201 to 1,333 mm, respectively. Annual average PET is generally higher than annual average rainfall. Therefore,

streamflow generation process in most of the divisions are controlled by water-limited environments (Milly et al.,

2005) except for the Tasmanian division (Table 2). Figure 2a shows the relationship of catchment area with record

length, while Fig. 2b shows the catchment area and the distribution of percentage of catchments, the distribution

170 is reasonably uniformly distributed in the range between 45 to 12,000 km² and slightly skewed outside this range.

Longest period of record is 69 years for several catchments having area from 14 to 15,850 km².

A quality-assurance, quality control (QA/QC) process was applied to observed time-series of daily streamflow

from each gauging station. This process identified and removed erroneous data values such as negative and

extreme values. The process of detection and removal was automated and then checked manually, as detailed in

175 Hydrologic Reference Station website (<http://www.bom.gov.au/water/hrs/references.shtml>). The GR4J model

(Perrin et al., 2003) was adopted to infill any missing data in accordance with the selection guidelines detailed in

Section 2.1. The mean and standard deviation of Nash-Sutcliffe efficiency for all 467 catchments was 0.74 and

0.12 respectively. As part of this process, a simple error correction procedure was used to ensure that initial and

final estimated flows matched adjacent observed values. This was done by linearly interpolating the start and end

180 of the infilled period to the observed flows. Through this process, a continuous quality-checked daily streamflow

time series was created for trend analyses.

Table 1 Total number of stations

Station features	Selection guidelines	Numbers
Existing stations decommissioned by February 2019	Passed	8
Existing stations operational and data up to February 2019	Passed	171
Existing stations operational and decommissioned	Failed	43
New stations operational and data up to February 2019	Passed	288
Total HRS stations	Passed	467

185

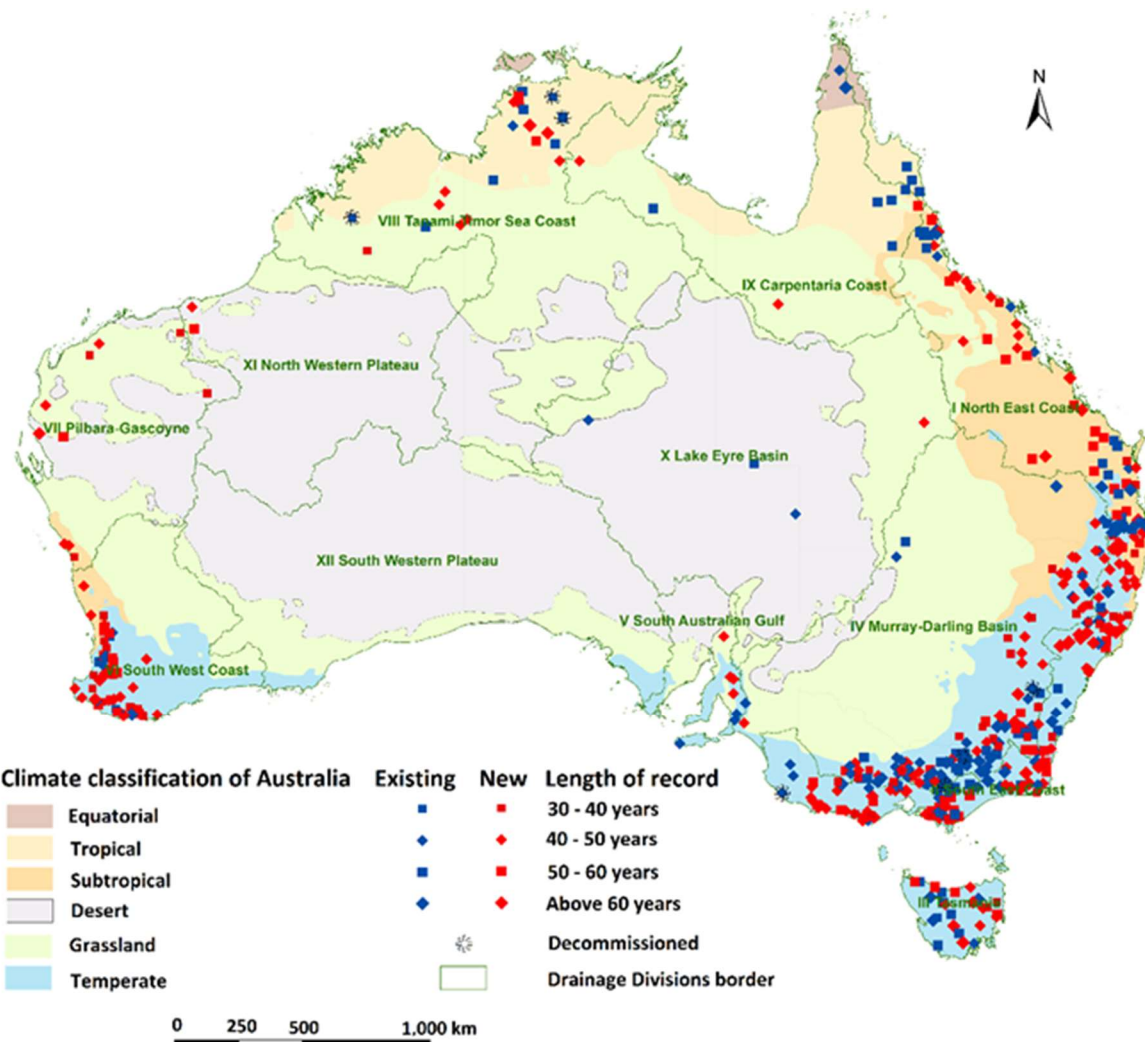
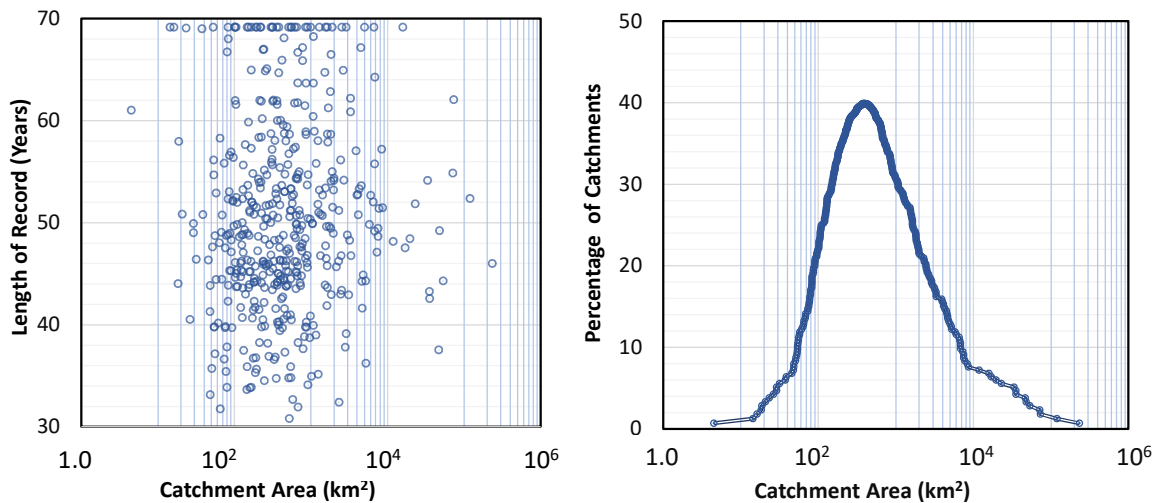


Figure 1. Map of Australia showing climate zones, Drainage Divisions and location of all gauges, new, existing, decommissioned, all scaled to length of record.



190

Figure 2. Length of record, catchment area and distribution of percentage of catchments for HRS

3 Methodology

Daily quality controlled and infilled daily data was accumulated to annual totals (based on water-year) and total for each of the four seasons. These five streamflow statistics formed the basis for trend analysis to capture annual 195 and seasonal trends. Seasons are defined as winter (June to August), spring (September to November), summer (December to February), and Autumn (March to May).

There are generally two types of changes often observed in streamflow data sets – long term persistent trend (monotonic) and sudden abrupt (step) change. Monotonic trends generally occur due to long term changes in rainfall, temperature and/or evapotranspiration, while step changes generally happen resulting from sudden 200 changes in flow generation thresholds. Statistical tests used to detect monotonic trends and step changes in streamflow generally fall into two categories – parametric and non-parametric tests.

202

203 Table 2: Metadata for Drainage Divisions and selected hydrologic reference stations

Division number	Drainage division	Mean annual rainfall (mm) (1950-2018)*	Mean annual PET (mm) (1950-2018)*	Mean elevation (m ASL)	Number of stations	Water-year start	Smallest catchment (km ²)	Largest catchment (km ²)	Infilled volume (%) (Mean/SD)	Missing data (%) (Mean/SD)
I	North East Coast	878	1855	173	66	October	16	35,326	0.7/1.7	0.5/1.0
II	South East Coast	885	1197	323	138	March	5	16,953	1.6/2.1	1.2/1.8
III	Tasmania	1333	853	199	25	February	18	3,285	0.7/1.1	0.8/1.3
IV	Murray-Darling Basin	484	1574	260	133	March	26	35,239	1.4/2.1	1.2/1.9
V	South Australian Gulf	313	1541	269	8	February	29	2,464	2.3/2.9	2.9/3.2
VI	South West Coast	439	1583	365	50	March	19	6,773	0.5/1.3	0.6/1.5
VII	Pilbara-Gascoyne	280	2098	162	10	September	907	72,902	0.1/0.2	0.1/0.2
VIII	Tanami-Timor Sea Coast	629	2152	339	21	September	65	47,652	5.2/2.8	6.0/6.0
IX	Carpentaria Coast	812	2143	293	10	October	333	8,638	4.1/2.9	5.5/3.2
X	Lake Eyre Basin	255	1849	312	4	October	3,324	232,846	0.1/0.2	0.9/0.9
XI	North Western Plateau	229	2115	359	2	September	6,503	53,323	5.6/5.2	4.3/3.2
XII	South Western Plateau	201	1773	297	0	(No data)	(No data)	(No data)	(No data)	(No data)

204 * Calculated from monthly gridded rainfall and PET data (5km by 5km) from AWAP (Raupach et al., 2009)

205

206

207

3.1 Trend analyses

We applied Theil Sen's approach (Sen, 1968; Theil, 1950), a non-parametric approach, to detect the magnitude of linear trend for each of the statistic (annual and four seasons total). In addition, trends were determined by using the non-parametric Mann–Kendall (MK) test (Kendall, 1975; Mann, 1945) because this technique is distribution-free, robust against outliers, and has a higher power for non-normally distributed data (Önöz and Bayazit, 2003; Yue et al., 2002). It has also been commonly used in streamflow trend analyses (Abdul Aziz and Burn, 2006; Birsan et al., 2005; Dixon et al., 2006; Lins and Slack, 1999). The Mann–Kendall test requires input data to be serially uncorrelated. Any serial correlation in the data structure can leads to overestimation of the significance of trends (Hamed and Ramachandra Rao, 1998; von Storch, 1995; Yue et al., 2002). To overcome the effect of serial correlation of higher order (namely Short-Term Persistence (STP)), two techniques are used here. These include: (i) Modified Mann–Kendall test, commonly known as Variance Correction (MK3) method as proposed by Hamed and Rao (1998), and (ii) Block Bootstrap (MK3bs) method (Kundzewicz and Robson, 2000). The MK3 and MK3bs approaches are more suitable when the time series shows higher order serial dependencies. Apart from Short Term Persistence (STP), the presence of Long-Term Persistence (LTP), or Hurst phenomenon, has been identified as a major source of uncertainty when analysing hydroclimatic data series (Koutsoyiannis, 2003; Kumar et al., 2009). To incorporate LTP behaviour in the Mann–Kendall test, the technique proposed by Hamed (2008) is used in this study. Using these three modified versions of Mann–Kendall test allows comparison of differences and check the validity of results for Australia. Non-parametric Pettitt test (Pettitt, 1979) and distribution free CUSUM test (Chiew, and Siriwardena, 2005) are generally used to detect abrupt step changes in streamflow. The Pettit test was used to detect step change for all five streamflow statistics, as it performs better than others for detecting step change and identifying change point (Villarini et al., 2009). Finally, the regional significance of any monotonic trends and step changes was tested using the Walker test (Wilks, 2006).

The Theil-Sen Slope approach, original Mann–Kendall (MK) test, three modified versions of the Mann–Kendall test, Pettitt Test and Walker test are briefly described in this section. Trend detection analysis may lead to misleading results when serial correlation (STP) and long-term persistence (LTP) in the streamflow data are ignored. The modified versions of Mann-Kendall tests, MK3, MK3bs and MK4 that account for STP, STP and LTP respectively are used to identify trends in streamflow data. A more detailed description can be found in Mann, 1945; Kendall, 1975; Hamed and Rao, 1998; Koutsoyiannis, 2003; Hamed, 2008; Pettitt, 1979; Wilks, 2006; Kumar et al., 2009; Zamani et al., 2017; Su et al., 2018; Kundzewicz and Robson, 2000).

We used Theil-Sen estimator and three different forms of Mann Kendall tests for monotonic trend analyses: (i) variance correction approach, (ii) Block Bootstrap approach and (iii) Long Term persistence.

3.1.1 Theil-Sen approach

The magnitude of trend is obtained using the Theil-Sen approach (Theil, 1950; Sen, 1968), where the magnitude of the slope of the trend is estimated as:

$$\beta = \text{Median} [(x_i - x_j)(i - j)]; \text{ for all } j < i \quad (1)$$

where x_i and x_j are streamflow data (annual and all seasons) at time points i and j, respectively. If the time series has n values, then there will be $N = n(n - 1)/2$ slope estimates and Theil-Sen slope β is taken as the median of these N values.

3.1.2 Independent Mann-Kendall (MK1) test

The Mann-Kendall test statistic (S) for a series $x_1, x_2, x_3, \dots, x_n$ is given by

$$S = \sum_{i=1}^{n-1} \sum_{j=i+1}^n sgn(x_j - x_i), \quad (2)$$

where

$$sgn(\theta) = \begin{cases} 1 & \text{if } \theta > 0 \\ 0 & \text{if } \theta = 0 \\ -1 & \text{if } \theta < 0 \end{cases} \quad (3)$$

The test statistic S is approximately normally distributed for $n \geq 8$ with zero mean. Variance as given as

$$V(S) = [n(n - 1)(2n + 5) - \sum_{i=1}^m (t_i - 1)(2t_i + 5)t_i]/18 \quad (4)$$

where m is the number of tied groups and t_i is the number of data in the i^{th} tied group. The standardised test statistic Z (standard normal distribution) is given as

$$Z = \frac{(S-1)}{\sqrt{V(S)}}; \quad \text{if } S > 0 \quad (5a)$$

$$Z = 0; \quad \text{if } S = 0 \quad (5b)$$

$$Z = \frac{(S+1)}{\sqrt{V(S)}}; \quad \text{if } S < 0 \quad (5c)$$

To identify and address the short term and long-term persistence in a streamflow series, we used three modified versions the of Mann Kendall test for monotonic trend analyses: (i) Variance Correction approach, (ii) Block Boot 260 Strap approach and (iii) Long Term persistence approach.

3.1.3 Mann-Kendall (MK3) test – Variance Correction Approach

This modified Mann-Kendall test, proposed by Hamed and Rao (1998), considers all the significant autocorrelation structure in a time series. The series x_i was ranked and autocorrelation coefficient of rank i of time series, was obtained to consider only the significant terms at 10% significance level. Autocorrelation 265 becomes insignificant after a lag of three (Rao et al., 2003). The effect of all significant autocorrelation coefficients in the dataset was removed by using a modified variance of S , described as $V(S)^*$ by

$$V(S)^* = V(S) \frac{n}{n^*} \quad (6)$$

where n^* represents the effective sample size. The $\frac{n}{n^*}$ ratio was computed directly from the equation proposed by Hamed and Rao (1998) as

$$\frac{n}{n^*} = 1 + \frac{2}{n(n-1)(n-2)} \sum_{i=1}^{n-1} (n-i)(n-i-1)(n-i-2)r_i \quad (7)$$

where n is the number of observations; and r_i is lag-i significant autocorrelation coefficient of rank i of time series. $V(S)^*$ is calculated using Eq. (6) and using $V(S)$ from Eq. (4). Finally, the Mann-Kendall Z was tested for significance of trend comparing it with threshold levels.

3.1.4 Mann-Kendall (MK3bs) test – Block Bootstrap (BBS) Approach

275 The Block Bootstrap (BBS) approach by Önöz and Bayazit (2012) was used to mitigate effects of serial correlation in datasets by performing bootstrapping (in blocks of data) so that the autocorrelation in the data is replicated. Data are resampled in blocks many times to estimate the significance of the observed Mann-Kendall test statistic S from the data sample while reflecting the serial correlation present in the dataset (Burn et al., 2016). Block length should be chosen so that data points in adjacent block are more or less independent. Khaliq et al. (2009)
 280 provide a detailed description of the steps involved in implementing the BBS approach.

In block bootstrapping, the simulation size N_s (the number of bootstrap samples to be generated in each case) and the block length L_b are the parameters whose values are to be chosen. The simulation size (N_s) is related to the level of significance required and the loss of power that can be allowed. Svensson et al. (2005) found that $N_s = 2000$ samples resulted in good stability in significance level estimates N_s . Block length chosen depends on 285 autocorrelation of the data, and should be larger than the *lag k* of the smallest significant autocorrelation coefficient R_i . Svensson et al. (2005) found that blocks of lengths of 5 were generally sufficient for most streamflow series.

Autocorrelation in time series varies across different sites, and Politis (2003) recommends the block length L_b is based on individual time series. To identify optimal block length L_b for individual annual and seasonal streamflow 290 time series, an automatic block length selection procedure proposed by Politis and White (2004) was used. The optimal block length obtained for annual and for each of the four seasonal streamflow time series for 467 gauging stations are shown in Fig. 3 below. In general, more than a third of the stations exhibit significant serial correlation of 2 or more ($L_b \geq 3$) and about 15% are serially uncorrelated ($L_b = 1$).

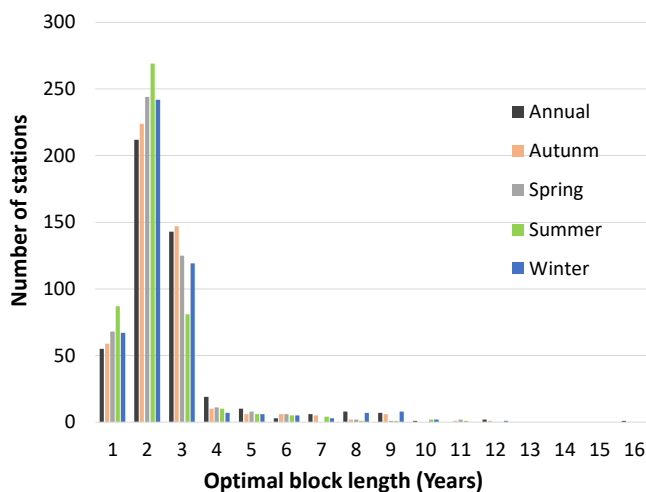


Figure 3: Optimal block length for annual and four seasonal streamflow time series for all 467 stations

295 We estimated the significance of the original Mann-Kendall test statistic S (Eq. 2) of the observed data from the simulated distribution, developed from resampled distribution of S from the moving block bootstrap procedure. Only if the original test statistic lies within the tails of the simulated distribution, the test statistic is likely to be significant (Do et al., 2017; Khaliq et al., 2009).

3.1.5 Mann-Kendall (MK4) test – Long Term Persistence (LTP)

300 This version of the Mann-Kendall method is proposed by Hamed (2008) and was described by Kumar et al. (2009) and it considers the Hurst coefficient, H , (Hurst, 1951) of a series for Long-Term Persistence (LTP). The coefficient H is used as a measure of long-term memory, i.e., autocorrelation of the time series. A value of 0.5 for H indicates a true random walk, which implies the time-series has no memory for previous values of observations. A value of H between 0.5 (0) and 1 (0.5) indicates a time-series with positive (negative) autocorrelation [e.g. an increase (decrease) between observations will probably followed by another increase (decrease)].

305

In this study, the following steps were carried out to apply the MK4:

1. Calculation of Hurst coefficient (H): A new trend free time series x'_i is calculated using

$$x'_i = x_i - (\beta \times i) \quad (8)$$

310 where β is the slope of a trend line using the Theil-Sen's approach and x_i is the streamflow data. Using the ranks of trend-free series [$x'_i: (i = 1: n)$] designated by R_i , the standardised Z_i variate (the equivalent normal variates of the ranks of de-trended time series) is computed as

$$Z_i = \varphi^{-1} \left(\frac{R_i}{n+1} \right) \quad (9)$$

315 where n is the number of streamflow data; and φ^{-1} is the inverse of the normal distribution function. Considering the hypothesis that the hydrometeorological processes exhibit scale invariant properties at any scale greater than annual (Koutsoyiannis, 2003), the elements of the Hurst matrix for a given H is computed as

$$C_n(H) = |\rho_{|j-i|}(H)| \quad \text{for } i = 1: n, j = 1: n \quad (10)$$

In the above equation $\rho_l(H)$ is lag- l autocorrelation coefficient for a given H and calculated by

$$\rho_l(H) = \frac{1}{2} (|l+1|^{2H} - 2l^{2H} + |l-1|^{2H}) \text{ for } l > 0 \quad (11)$$

320 The log-likelihood function of n Normal observations with a scaling coefficient H is given by Eq. (12) (McLeod and Hipel, 1978), where the accurate value of H can be computed by maximising the function of H as follows:

$$\log L(H) = -\frac{1}{2} \log |C_n(H)| - \frac{Z^T |C_n(H)|^{-1} Z}{2\gamma_0} \quad (12)$$

325 In the above equation, Z^T is the transpose of vector Z obtained from Eq. (9); γ_0 equates the variance of Z_i and $C_n(H)$ and $C_n(H)^{-1}$ are Hurst matrix and inverse of the Hurst matrix, respectively. These two last matrices can be obtained using Eq. (10). To maximise $\log L(H)$, H is assumed to be in the range of 0.5–0.98 and the mentioned function is computed for a given H . The procedure is repeated for other H values with 0.01 steps. The H value producing the maximum value of $\log L(H)$ is taken as the answer.

2. Mean and standard deviation of H : According to Hamed (2008), the mean and standard deviation of H are expressed as a function of n as follows:

$$\mu_H = 0.5 - 2.87n^{-0.9067} \quad (13)$$

$$\sigma_H = 0.77654n^{-0.5} - 0.0062 \quad (14)$$

Then Z_{cal} is calculated as

$$z_{cal} = \frac{H - \mu_H}{\sigma_H} \quad (15)$$

335 This Z_{cal} , obtained from Eq. (15) was tested for significance of trend at the 10% significance level. The MK4 procedure was continued if Z_{cal} was greater than the critical normal value (1.645), otherwise the procedure for independent Mann-Kendall (MK1) test was adapted as the LTP is not significant.

3. Significant H values (LTP is significant): The modified variance for the S statistic was computed as recommended by Kumar et al. (2009) and Hamed (2009) as:

$$340 \quad V(S)^{H'} = \sum_{i=1}^{n-1} \sum_{j=i+1}^n \sum_{k=1}^{n-1} \sum_{l=k+1}^n \frac{2}{\pi} \sin^{-1} \left(\frac{\rho|j-l| - \rho|i-l| - \rho|j-k| + \rho|i-k|}{\sqrt{(2-2\rho|i-j|)(2-2\rho|k-l|)}} \right) \quad (16)$$

In the above equation ρ_l is calculated using Eq. (11) for a given value of H. Since $V(S)^{H'}$ is a biased estimator, we have corrected it for bias using

$$V(S)^H = V(S)^{H'} \times B \quad (17)$$

where B is expressed as a function of sample size, n , as follows (Hamed 2008; Kumar et al. 2009):

$$345 \quad B = a_0 + a_1H + a_2H^2 + a_3H^3 + a_4H^4 \quad (18)$$

$$a_0 = \frac{1.0024n - 2.5681}{n + 18.6693} \quad (19a)$$

$$a_1 = \frac{-2.2510n + 157.2075}{n + 9.2245} \quad (19b)$$

$$a_2 = \frac{15.3402n - 188.6140}{n + 5.8917} \quad (19c)$$

$$a_3 = \frac{-31.4258n + 549.8599}{n - 1.1040} \quad (19d)$$

$$350 \quad a_4 = \frac{20.7988n - 419.0402}{n - 1.9248} \quad (19e)$$

When using the MK4 method, $V(S)^H$ obtained from Eq. (17) was used as $V(S)$ in Eq. (5) of the MK1. The significance of Z was then tested for significance of a trend.

3.2 Pettitt test for step change

We used the non-parametric Pettitt test (Pettitt, 1979) to detect step changes in annual and seasonal streamflow. 355 This procedure is least sensitive to outliers, and skewed distributions of the streamflow datasets in comparison to other methods used for detecting step changes, makes it most suitable for this analysis (Sagarika et al., 2014). This test can identify anomalies in the mean and, or, median streamflow when the time of step change is unclear. It uses a version of the Mann-Whitney statistics to quantify the significance of probabilities by testing two samples

from the same population. In the Pettitt test the p-value is computed in a manner that adjusts for the fact that the
360 method is designed to find the most advantageous point in the record to consider as the change point (Helsel et al., 2020; Villarini et al., 2009).

Using Pettitt (1979), let us assume n to be the length of the time series and τ to be the year of the step change. Viewing the time series as two samples x_1, \dots, x_τ and $x_{\tau+1}, \dots, x_n$, an index, V_τ can be defined as:

$$V_\tau = \sum_{j=1}^n \operatorname{sgn}(x_\tau - x_j) \quad (20)$$

365 where $\operatorname{sgn}(x)$ is the same as $\operatorname{sgn}(\theta)$ in Eq. (3) and U_τ is defined in Equation (21).

$$U_\tau = \sum_{i=0}^\tau V_i \quad (21)$$

When a significant step change exists in a time series, a graph between $|U_\tau|$ and τ increases up to the step change point and then decreases again, or vice versa. However, in the absence of a step change point, the graph would continually increase or decrease to the end of the time series. The most significant step change point τ is
370 established at the point where $|U_\tau|$ is maximum, given as K_n and defined by

$$K_n = \max_{1 \leq t \leq n} |U_\tau| \quad (22)$$

In a year where $|U_\tau|$ is the maximum, the significance probability associated with K_n is approximated by

$$p = 2 e^{\left(\frac{-6K_n^2}{n^3+n^2}\right)} \quad (23)$$

where the approximation holds and is accurate to two decimal places, for $p < 0.5$ (Pettitt, 1979).

375 In this study, we adopted a significance level of $p \leq 0.10$, and evaluated the direction of change. The minimum value of U_τ , extracted by K_n indicates positive change, and a maximum value indicates a negative change.

3.3 Test for regional significance

We assessed the regional significance of trends detected at a local point scale to examine if similar trends were also detected at neighbouring locations. The main objective is to assess whether a certain minimum number of
380 locations with significant trends occur at a regional scale to make it field significant or not. The test for regional significance is rather conservative, as it is based on a null hypothesis of independent trends across stations, when the trends within a region are positively correlated. We applied Walker's test (Wilks, 2006; Sagarika et. al., 2014) in detecting regional significance of monotonic and step changes in streamflow time series – for annual total and across the four seasons at a 90% confidence level ($p \leq 0.10$) for all 467 stations across Australia.

385 The Walker's test considers a set of K independent MK and Pettitt tests, all of whose null hypothesis are assumed to be true (i.e. corresponding p-values are assumed uniformly distributed as $U(0, 1)$). We further assume that $p_{(1)}$ is the smallest of the p value set. In this case, the probability distribution $p_{(1)}$ is given by

$$f[p_{(1)}] = \frac{K!}{(1)!(K-1)!} p_{(1)}^0 [1 - p_{(1)}]^{K-1} \quad 0 \leq p_{(1)} \leq 1 \quad (24)$$

$$f[p_{(1)}] = K[1 - p_{(1)}]^{K-1} \quad (25)$$

390 To reject the global null hypothesis that all K local null hypotheses are true (i.e., to declare field significance), p_1 must be no larger than a critical value p_{walker} . The critical value for this global test can be obtained using

$$\alpha_{global} = K \int_0^{p_{walker}} [1 - p_{(1)}]^{K-1} dp_{(1)} \quad (26a)$$

$$\alpha_{global} = 1 - (1 - p_{walker})^K \quad (26b)$$

$$p_{walker} = 1 - (1 - \alpha_{global})^{1/K} \quad (27)$$

395 A global null hypothesis may be rejected at the α_{global} (0.10) level if the smallest of K independent local p value is less than or equal to p_{walker} .

4 Results

For water year and the four seasons, monotonic trend considering short-term (STP) and long-term (LTP) persistence and the step changes were evaluated at a significance level of $p < 0.10$ for each streamflow station. 400 The water year begins in September/October for the northern part of Australia (drainage divisions I, VII, VIII, IX, X) and in February/March for the southern part of the country (drainage divisions II, III, IV, V, VI) (Fig. 1, Table 1). We undertook trend analysis for annual and seasonal streamflows in these two regions of Australia separately.

4.1 Linear trends

405 4.1.1 Theil-Sen approach

Box plots of trend slopes estimated by Theil-Sen's approach for annual and seasonal streamflow in southern and northern divisions that are significant are shown in Fig. 4. For example, the trend slope for a site in South Esk River in Tasmania is shown in Fig. 5a, where the decrease in annual streamflow is 5.91 GL/year (1.8 mm per year per year). For drainage divisions in the south, the medians of slopes for all annual and seasonal streamflows were 410 less than zero. The lowest trend line slope (-2.07 mm per year per year) occurred in spring (Sep-Nov) and the median of slopes in autumn (Mar-May) is less negative than the other three seasons in the southern parts of Australia (Fig. 4a). Streamflow in all four seasons showed a downward trend in the southern divisions. Approximately 60% of annual streamflow volumes in the southern drainage divisions occur in winter and spring (between Jun-Nov). For annual flows in the south, slopes were between -6.5 to -0.07 mm per year per year 415 (Fig. 4a) and the median of slopes was approximately -1.79 mm per year per year.

Medians of slopes for annual and seasonal streamflow were located close to, or above zero for drainage divisions in the northern part of Australia (Fig. 4b). The highest (+7.13 mm per year per year) trend line slope occurred in the summer (Dec-Feb). The median of trend line slopes in summer (+1.02 mm per year per year) is higher than that in the other three seasons (all <0.01 mm per year per year) in the northern divisions. Streamflow in all seasons, except in summer, showed negligible trends in northern parts of Australia. More than 90% of the annual streamflow volumes in the northern drainage divisions occur in summer and autumn (between Dec-May). For 420

annual flows, slopes were between +12.1 and -6.0 mm per year per year (Fig. 4b) and the median of slopes was approximately +1.46 mm per year per year. Fig. 5a shows a typical example of linear trend analysis using Theil Sen's approach for annual streamflow in southern Australia.

425

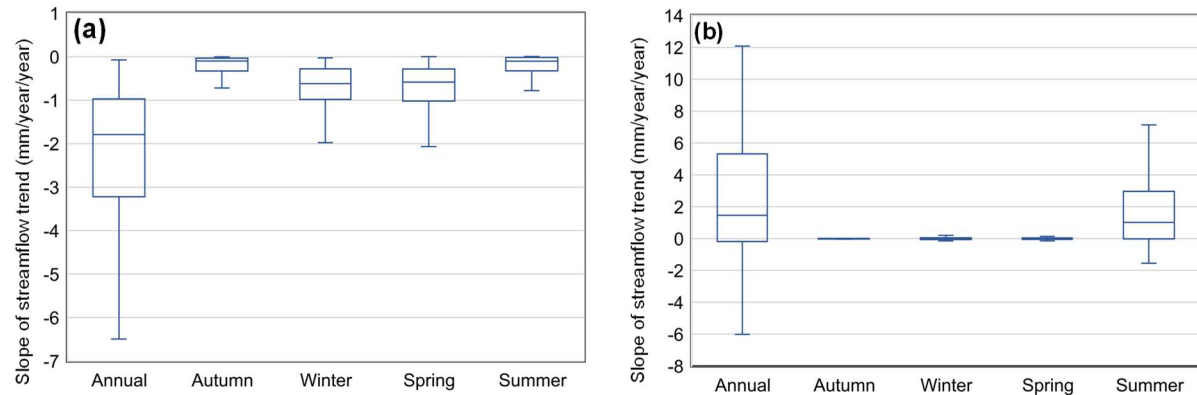
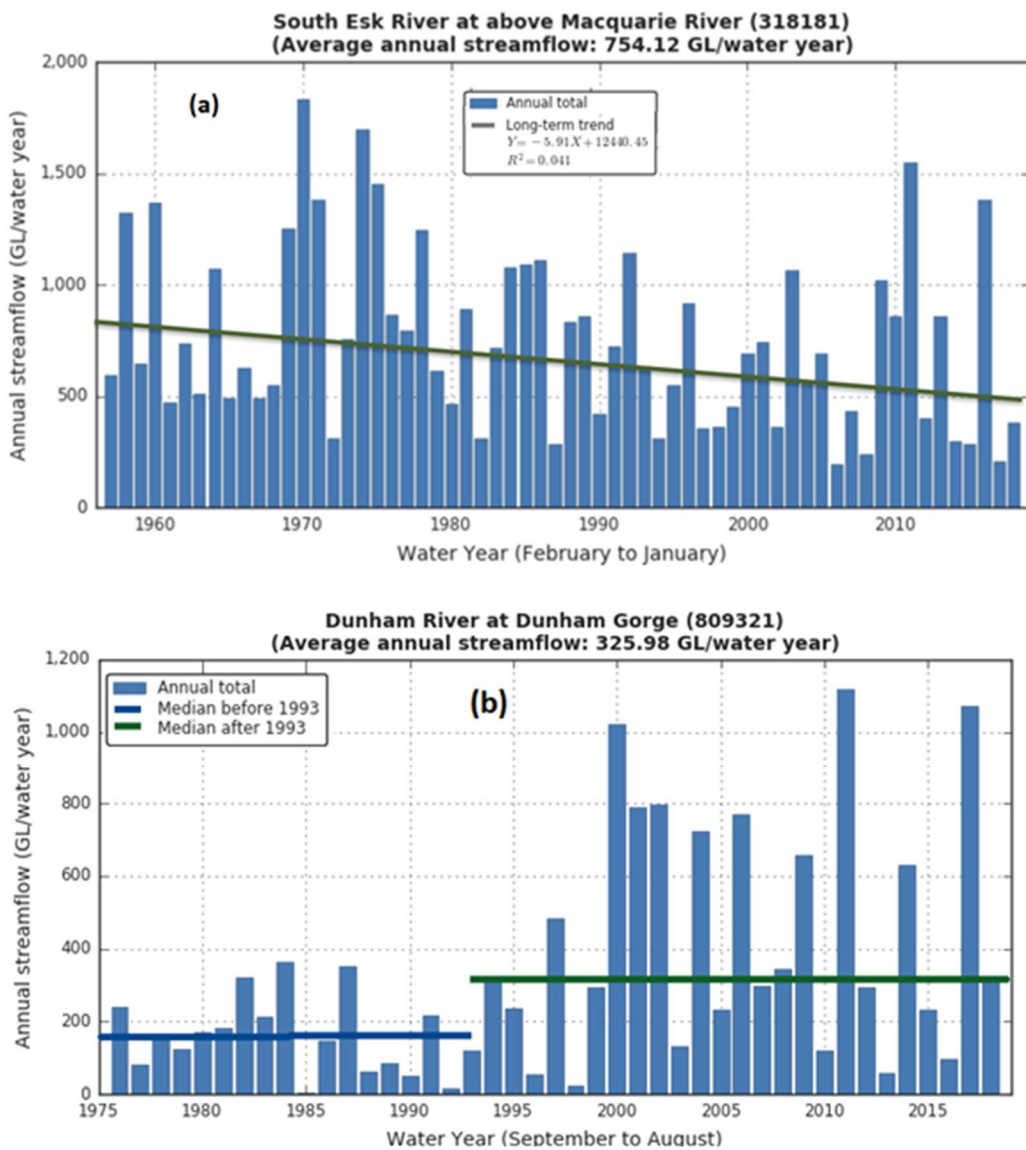


Figure 4: Box plot of Theil-Sen's slope in mm/year/year for annual and seasonal streamflow for drainage divisions in (a) Southern and (b) Northern Australia



430 **Figure 5: Typical examples of (a) trend and (b) step change in annual streamflow in southern and northern Australia**

4.1.2 Monotonic trend – the Short (STP) and Long (LTP) Term Persistence

Streamflow data from stations that are significantly autocorrelated (lag-1 or more) at $p < 0.10$ and H values that are significant at $p < 0.10$ are considered to have short-term (STP) and long-term (LTP) persistence, respectively.

435 To analyse the presence of STP and LTP, results from the MK3 and MK4 tests were examined respectively. In the South East Coast (II), South West Coast (VI) coasts and southern Murray-Darling Basin (IV), most stations showed significant STP or LTP, or both STP and LTP for the water-year and for all four seasons (Fig. 6). Across water years and all seasons, the percentage of stations with STP was greater than those with only LTP or both STP and LTP. For water years, data from 88% of stations showed STP and 28% showed LTP across Australia.

440 However, LTP was evident mainly in the southern and south-eastern parts of Australia (divisions II, III, IV, V, VI) and in the north in the Carpentaria Coast (IX). Seasonally, autumn had the highest number of stations (221) with LTP persistence.

Data from stations with significant correlation at $p < 0.10$ in STP and LTP were tested for trends (Table 3) using MK3 and MK4 tests, respectively. Of the 412 stations with significant STP across water years, 196 stations showed trends from the MK3 test. Of 130 stations with data showing significant LTP, 14 had significant trends from the MK4 test. In drainage divisions II to VI in the south, nearly half of stations showed significant trends with STP. However, results vary slightly across different drainage divisions for the four seasons. In autumn, 33% of the 87% of stations with significant STP showed trends, while 6% of the 47% of stations with significant LTP showed trends. Similarly, in winter, 39% out of 86% of stations with STP, showed trends, while 3% of the 27% of stations with LTP, showed trends. In spring, 44% of the 85% of stations with significant STP, showed trends while 2% of the 24% of stations with significant LTP, showed trends. In summer, 36% of 81% of stations with significant STP, showed trends while 3% of 19% of stations showing LTP, showed trends.

Table 3 Summary of stations with short-term persistence (STP) and long-term persistence (LTP) of streamflow, and stations that showed trends under MK3 and MK4 tests across drainage divisions for water year and the four seasons at $p \leq 0.10$.

Drainage division	Drainage division name	Water year		Autumn		Winter		Spring		Summer	
		STP/ Trend	LTP/ Trend								
I	North East Coast (66)	59/4	23/0	57/2	18/0	51/18	31/1	60/15	22/0	46/5	9/0
II	South East Coast (138)	124/62	71/8	122/45	54/7	115/37	43/4	112/70	51/6	114/58	32/5
III	Tasmania (25)	21/13	0/0	23/11	0/0	20/10	0/0	21/7	0/0	21/9	0/0
IV	Murray-Darling Basin (133)	117/74	28/4	115/60	100/14	120/70	23/3	115/85	11/2	119/47	27/3
V	South Australian Gulf (8)	8/4	0/0	8/3	5/1	8/2	0/0	8/5	0/0	5/4	3/0
VI	South West Coast (50)	42/26	4/2	44/28	23/8	45/29	3/2	41/19	3/0	39/25	15/5
VII	Indian Ocean (10)	7/1	0/0	9/3	1/0	9/7	1/0	9/2	7/0	9/5	2/1
VIII	Tanami-Timor Sea Coast (21)	19/10	1/0	16/1	13/0	16/6	16/3	17/10	8/1	15/12	0/0
IX	Carpentaria Coast (10)	9/1	3/0	9/0	4/0	10/1	8/1	10/2	5/0	7/2	1/0
X	Lake Eyre Basin (4)	4/1	0/0	3/1	2/0	4/2	1/0	4/0	1/0	3/2	1/0
XI	North Western Plateau (2)	2/0	0/0	2/0	1/0	2/1	1/0	2/1	2/0	2/0	0/0
XII	South Western Plateau (0)	---	---	---	---	---	---	---	---	---	---
Total		412/196	130/14	408/154	221/30	400/183	127/14	399/216	110/9	380/169	90/14

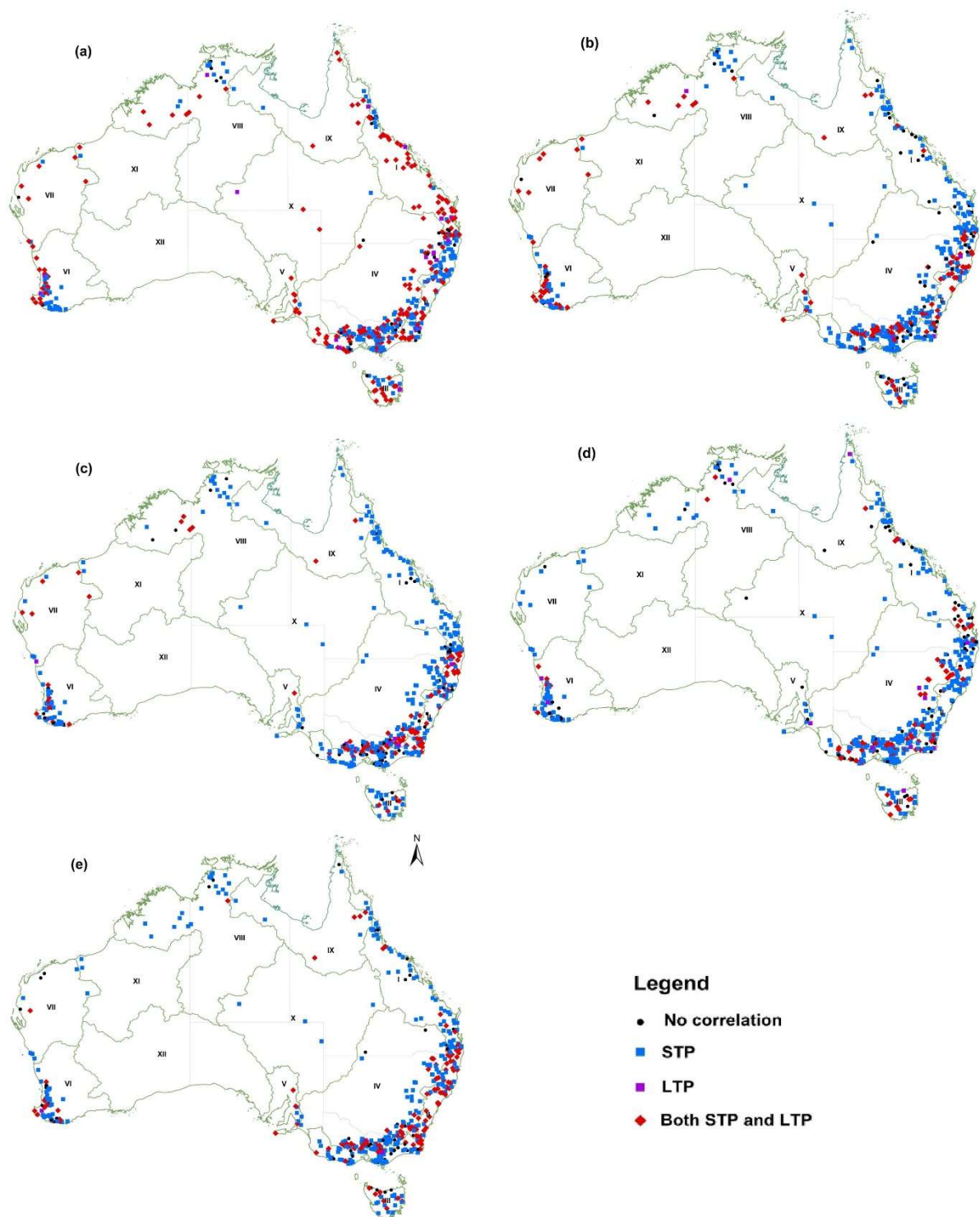


Figure 6: Spatial distribution of stations where streamflow shows persistence, Short Term (STP) and Long Term (LTP), in (a) autumn (Mar-May), (b) winter (Jun-Aug), (c) spring (Sep-Nov), (d) summer (Dec-Feb), and (e) annual (water year) at $p < 0.10$.

460

4.1.3 Monotonic trends - MK tests

Table 4 summarises the MK3, MK3bs and MK4 test results. Fig. 7. show the distribution of trends for each drainage division for the water year, autumn, winter, spring, and summer for all three MK tests. The MK3 test

results are similar to the MK3bs test results for water years and all four seasons, as they both consider the full autocorrelation structure (STP) of the streamflow series. Spatial distribution of trends under all three MK tests in the water year suggests the annual mean streamflow has increased in Tanami-Timor Sea Coast division in northern Australia and decreased in the southwest and southeast parts of the country (Fig. 7). Magnitude trends in streamflow volumes expressed by Theil-Sen's slope show a maximum of 2.4 %/year increase at one station in the Tanami-Timor Sea Coast (VIII) and a maximum decrease of -3.9 %/year at one station in the Murray-Darling Basin (IV) over a period of at least 50 years. The MK3 test results are almost like that of MK3bs test for water years and all four seasons, as they both consider the full autocorrelation structure (STP) of the streamflow series. Therefore, MK3 test results are initially analysed.

Though most of all 467 streamflow stations showed trends, across water years, only 14 stations had data with increasing trends, and 212 stations showed decreasing trends that were statistically significant (Table 4). In the water year, more than 50% of stations in the drainage division with increasing trends was the Tanami-Timor Sea Coast (VIII). Streamflows that showed decreasing trends were within the South East Coast (II), Tasmania (III), Murray-Darling Basin (IV), South Australian Gulf (V) and South West Coast (IV) drainage divisions. Most stations in other divisions showed no significant trend (Fig.7)

For autumn (Mar-May), streamflows at more than 50% of stations showed significant trends in the South East Coast (II), Tasmania (III), Murray-Darling Basin (IV), South Australian Gulf (V) and South West Coast (IV) and North East Coast (I) divisions. Other divisions showed autumn decreasing trends that were very similar to those found across water years, except for the Tanami-Timor Sea Coast (VIII) in the north, where only one station showed an increasing trend. Data from 173 stations showed significant trends across water years, 4 out of which were increasing and 169 were decreasing (Table 4). In autumn, the maximum increase in streamflow was 1.3%/year, and the maximum decrease was -5.8%/year. Both trends were at stations in South West Coast (IV).

Across winter (Jun-Aug), streamflows at over half of the stations showed significant decreasing streamflow trends in the North East Coast (I), Tasmania (III), Murray-Darling Basin (IV), and South West Coast (IV) and significant increasing trends in the Tanami-Timor Sea Coast (VIII). However, in the South East Coast (II), Pilbara-Gascoyne (VII), Carpentaria Coast (IX) and the Lake Eyre Basin (X), fewer than 50 % of stations had flows with significant trends. A total of 189 stations showed significant trends (for MK3) in streamflows across Australia, of which 9 are increasing, and 180 are decreasing trends (Table 4). The maximum increase in winter flows was 2.3 %/year (in the Tanami-Timor Sea Coast (VIII)) and the maximum decrease was -3.4 %/year (in the Murray-Darling Basin (IV)). For stations in the Murray-Darling Basin (IV), significant trends vary between -0.5 % and -3.4 % (median of -1.3%/year).

Spring (Sep-Nov) saw more stations with decreasing flow trends compared with water years or the other seasons. Trends in flow were mostly detected at stations in all divisions except for Lake Eyre Basin (X) and North Western Plateau (XI), for which there is very limited flow data. South East Coast (II) and Murray-Darling Basin (IV) divisions had the highest number of stations with decreasing trends in streamflow, compared with trends in the water year and other seasons (Table 4). There were stations in the South East Coast (II), Tasmania (III), Murray-Darling Basin (IV) and South Australian Gulf (V) that showed significant decreasing trends. For spring (Sep-Nov), 235 stations showed significant trends – 8 increasing and 227 decreasing (Table 4). The maximum increase

in spring flows was 3.1 %/year (in the Tanami-Timor Sea Coast (VIII)), and the maximum decrease was -2.8 %/year respectively (in the South West Coast (IV) divisions.

For summer (Dec-Feb), stations in the Tanami-Timor Sea Coast (VIII) showed significant increasing flow trends as with trends in other seasons. Stations in the South East Coast (II), Tasmania (III), Murray-Darling Basin (IV), South Australian Gulf (V) and South West Coast (VI) divisions showed significant decreasing trends in flow. In summer, 175 stations showed significant flow trends – 26 increasing and 149 decreasing (Table 4). The maximum increase in summer flows was -2.1%/year (in the Tanami-Timor Sea Coast (VIII)) and the maximum decrease was -5.0%/year (in the South West Coast (IV) division.

While results from the MK3 and MK3bs tests are nearly identical for most cases, MK3 and MK4 do show differences for most annual and seasonal flow statistics. A typical example of MK3bs statistic obtained from 2000 samples of two locations with a) decreasing and b) increasing trends is shown in Fig. 8. It illustrates how the observed values are located below or above 5th and 95th percentiles respectively. A small number of stations have significant trends in streamflow when LTP behaviour (MK4) was considered (Fig. 7, Table 4). This is particularly evident in South East Coast (II) for water years, and in the Murray-Darling Basin (IV) for autumn (Table 4, Fig. 7). The MK4 test resulted in more stations with trends in winter and spring, compared to autumn and summer. Across Australia for water years, 14 stations showed significantly increasing trends in flow, and 196 stations showed significantly decreasing trends, slightly less than MK3 and MK3bs test results (Table 4). Similar results are also evident for four seasons across Australia (Table 4).

Table 4 Results of three Mann Kendall (MK) tests for water year and all four seasons

Drainage division	Drainage division name	Water year			Autumn			Winter			Spring			Summer		
		MK3 +/-	MK3bs +/-	MK4 +/-												
I	North East Coast	0/4	0/9	0/2	1/2	0/2	0/2	3/10	2/11	2/9	3/11	2/12	2/11	0/6	0/6	0/6
II	South East Coast	0/64	0/64	0/54	0/58	1/60	0/40	0/42	0/38	0/41	0/77	0/77	0/69	0/58	0/58	0/50
III	Tasmania	0/15	0/13	0/15	0/16	0/15	0/16	0/12	0/13	0/13	0/8	0/7	0/7	0/9	0/9	0/9
IV	Murray-Darling Basin	0/89	0/82	0/84	0/61	0/67	0/32	0/75	0/76	0/70	0/98	0/92	0/93	1/48	0/46	0/42
V	South Australian Gulf	0/5	0/3	0/5	0/3	0/4	0/2	0/3	0/3	0/3	0/5	0/3	0/5	1/5	0/4	0/4
VI	South West Coast	0/33	0/33	0/34	1/27	3/28	1/26	0/33	0/32	0/33	1/22	1/23	1/21	5/22	5/20	5/21
VII	Pilbara-Gascoyne	1/1	1/1	1/1	1/1	1/1	1/1	0/4	0/5	0/4	1/2	1/2	0/0	2/2	2/0	2/0
VIII	Tanami-Timor Sea Coast	12/0	11/0	12/0	1/0	1/0	0/0	5/0	6/0	4/0	2/4	4/1	2/1	14/0	13/0	13/0
IX	Carpentaria Coast	1/0`	1/0`	1/0`	0/0	1/0	0/0	1/1	1/1	1/0	1/1	1/1	0/1	2/0	2/0	2/0
X	Lake Eyre Basin	0/1	0/1	0/1	0/1	0/1	0/0	0/1	0/1	0/1	0/0	0/0	0/0	1/1	1/1	1/0
XI	North Western Plateau	0/0	0/0	0/0	0/0	0/0	0/0	0/0	0/0	0/0	0/0	0/0	0/0	0/0	0/0	0/0
XII	South Western Plateau	---	---	---	---	---	---	---	---	---	---	---	---	---	---	---
	Total	14/212	13/206	14/196	4/169	7/178	2/119	9/180	9/180	7/174	8/227	9/218	5/208	26/149	23/144	23/131

MK3, MK3bs, MK4 correspond to MK tests

+ Number of stations showing increasing trends

- Number of stations showing decreasing trends

525 Entries in bold indicate results that are field significant at $p < 0.10$.

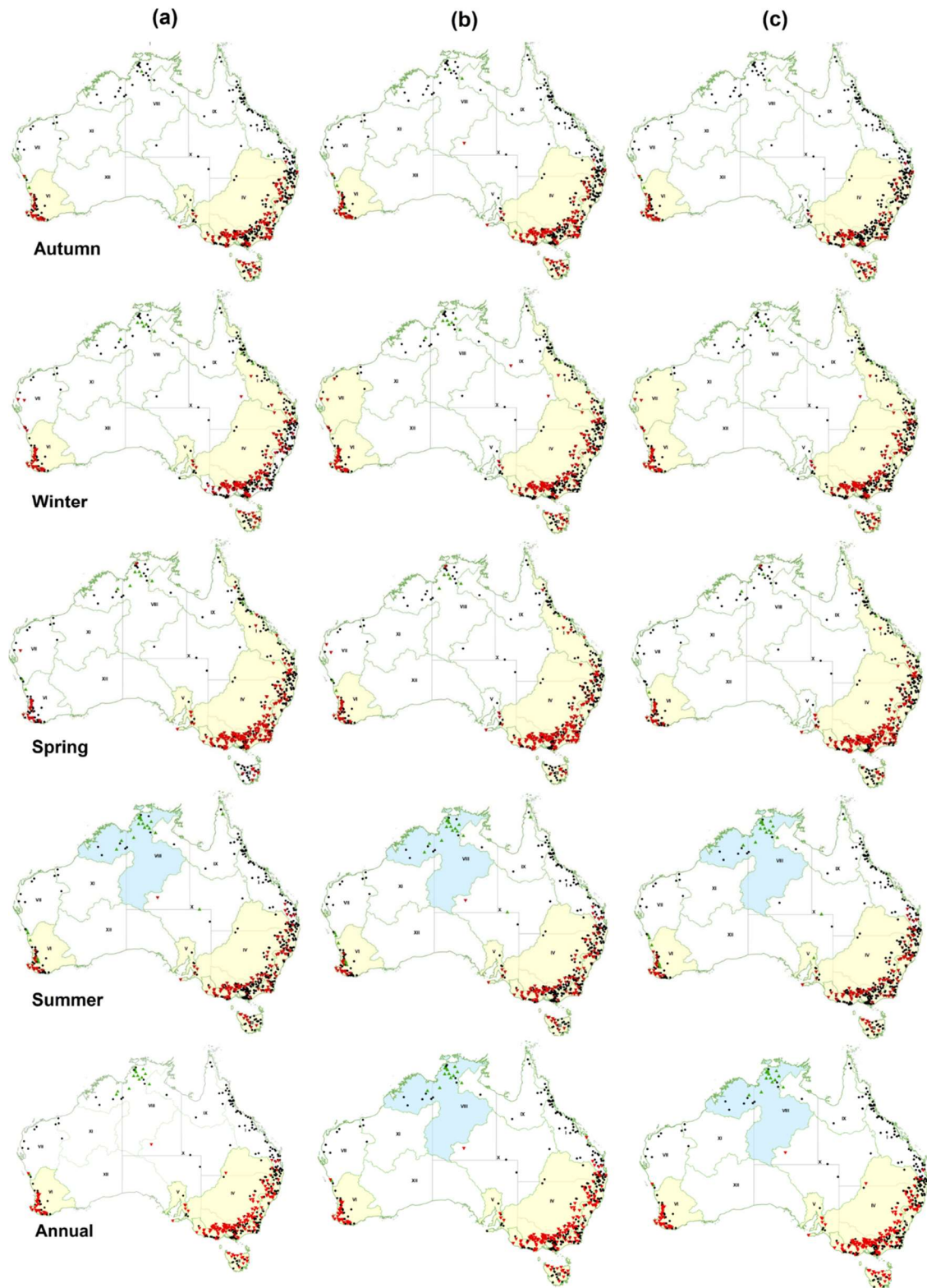
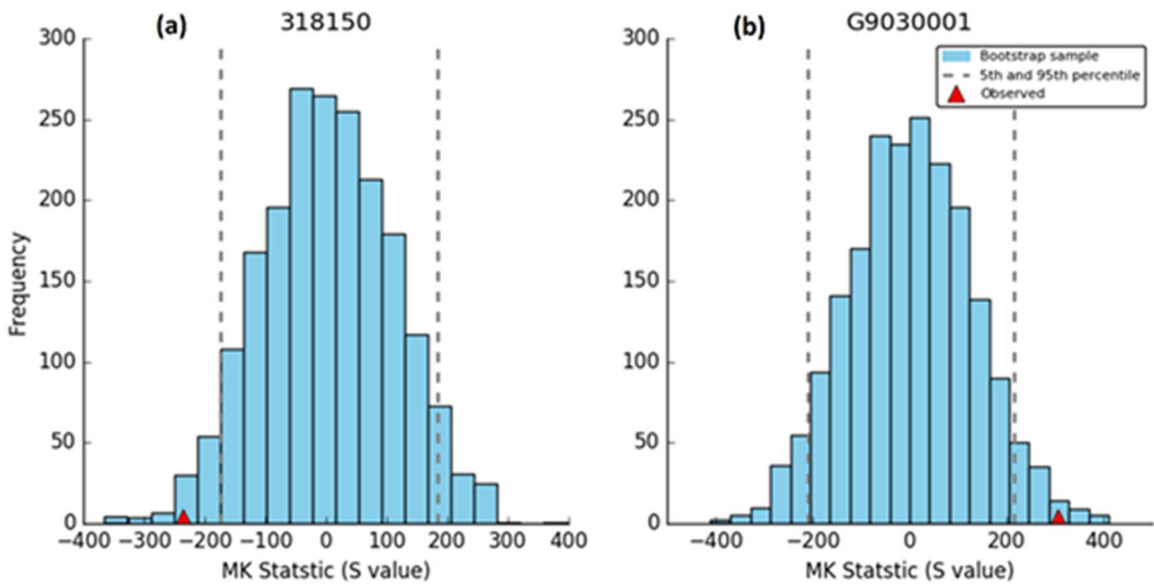


Figure 7: Maps showing seasonal trends using (a) MK3, (b) MK3bs, and (c) MK4 tests. Results are reported for autumn, winter, spring, summer, and annual (water year) ($p < 0.1$). Upward-pointing triangles (green) indicate significant increasing trends, and downward-pointing triangles (red) indicate significant decreasing trends. Grey dots indicate stations with no trends. Drainage divisions with positive and negative trends with field significance at $p < 0.10$ are coloured blue and yellow, respectively.



535 **Figure 8: Examples of histograms for two stations representing the frequency distribution of MK Statistic (S) obtained from 2000 samples of moving-block bootstrap iterations; red triangles are observed values, while dotted lines show the 5th and 95th percentiles for (a) decreasing trend (318150) and (b) increasing trend (G9030001) in Tasmania (III) and Carpentaria Coast (IX) divisions, respectively**

4.2 Step change

540 The non-parametric Pettitt test (Pettitt, 1979) was used to test for step changes for water years as well as for all seasons. This test is biased towards finding step changes in the centre of a time series (Mallakpour and Villarini, 2016). As the annual streamflow has a skewed distribution and possibly have outliers, this non-parametric test, which is least sensitive to these characteristics, is well suited to change point detection. A typical example of step change in northern Australia is shown in Fig. 5b. Step change maps (Fig. 9a) clearly reveal a spatial pattern in the
 545 location of stations that exhibited a significant step change in flow. The direction and significance of step changes are consistent with results from MK tests (Fig. 7) for most stations. Years when step changes occurred show spatial groupings within several drainage divisions. Significant step changes or shifts across water years, and all four seasons for each drainage division are summarised in Table 5. For water years, the South East Coast (II), Murray-Darling Basin (IV), South Australian Gulf (V), South West Coast (VI) and Tanami-Timor Sea Coast
 550 (VIII) drainage divisions all showed significant step changes for more than 60% of station flows (Fig. 9a, Table 5). Increasing shifts were seen in northern Australia, including the Indian Ocean (VII), Tanami-Timor Sea Coast (VIII) and Carpentaria Coast (IX) divisions, whereas decreasing shifts were seen in all drainage divisions except for the Tanami-Timor Sea Coast (VIII), Carpentaria Coast (IX) and North Western Plateau (XI). The South East Coast (II), Murray-Darling Basin (IV), South West Coast (VI) and Tanami-Timor Sea Coast (VIII) had significant step changes across water years (Fig. 9).

For summer (Dec-Feb), the lowest proportion of stations had significant step changes in flow compared with the other seasons or with water years (Table 5). The South East Coast (II), Murray-Darling Basin (IV) and South

West Coast (VI) divisions had significant step changes at $p < 0.10$ for water years and for all seasons, while Tanami-Timor Sea Coast (VIII) step changes for water years and all seasons except for autumn. Tasmania (III) had significant step changes only in autumn. North East Coast (I) had significant step changes in spring and winter. South Australian Gulf (V) had significant step changes in autumn and winter (Fig. 9).

Figure 9 shows the number of stations with step changes in flow, each year between 1950 and 2018 for water years, and for each season. The first step change was detected in 1964, and most changes occurred between 1970 and 1999. Out of 467, a total of 253 stations show step changes in flows for water years ($p < 0.10$) of which 16 were increasing and 237 were decreasing changes in flows. Water years between 1992 and 2004 had increasing step changes in 16 stations, with the water-year 1996 having 9 stations with increasing step changes in flow (Fig. 9b). The period from 1975 to 1979 showed decreasing step changes for 24 stations; out of which 18 were in the 1978 water year. The period from 1981 to 1989 show decreasing step changes for 8 stations, and the period from 1990 to 2000 showed decreasing step changes in 190 stations, half of which occurred in the 1996 water year.

Autumn (Mar-Jun) had a total of 210 stations with step changes ($p < 0.10$) in flow, of which 8 were increasing and 202 decreasing. The first increasing step change in autumn was detected in 1970 (Fig. 9b), in the Carpentaria Coast (IX) division. Similar to water years, most step changes occurred between 1990 and 2000, with 147 stations showing decreasing step changes in flow (Table 5). About quarter of the step changes took place in the 1996 water year.

In winter (Jun-Aug) 246 stations showed a step change ($p < 0.10$) in flow, of which 16 were increasing and 230 decreasing. The first step change in winter occurred in 1970 (Fig. 9b). One station showed increasing shifts starting early in the 1970s, and 10 additional stations during 1996 to 1999. During the period from 1975 to 1982, 10 stations showed decreasing step changes in flows. Between 1990 and 2000, 211 stations (the largest in total), showed a decreasing step change in flows, with 101 of these changes occurring in 1996.

Spring (Sep-Nov) had a total of 219 stations with step changes ($p < 0.10$) in flow, of which 21 stations had an increasing step change and 198 stations had a decreasing shift. The period from 1994 to 1997 saw 11 stations with increasing step changes (Fig. 9b) and in the period from 1989 to 2001, 178 stations had decreasing step changes in their spring flows.

Summer had a smaller number of stations (160 out of 467) with step changes ($p < 0.10$) in flows, of which 24 stations had increasing shifts and 136 stations had decreasing step changes (Table 5, Fig. 9b). The distribution of stations with step changes varied across the period of record; with 28 stations with decreasing step changes during 1976-1989, 4 stations increasing during 1980-1988, 101 stations decreasing during 1992-2002 and 18 station increasing during 1990-2000 (Fig. 9b).

Fig. 10 shows the timing of step changes for several drainage divisions where the water-year range mostly from 1976 to 2009. The period from 1990 to 2000 showed decreasing step changes for 199 stations, mostly in the South East Coast (II), Murray-Darling Basin (IV) and South West Coast (VI) divisions. Most increasing step changes are in the Tanami-Timor Sea Coast (VIII) division during 1992-1998. The South East Coast (II), Murray-Darling Basin (IV), South West Coast (VI) and Tanami-Timor Sea Coast (VIII) divisions showed a greater number of stations with step changes distributed across the study period, indicating a higher association to natural changes and climate variability than for other regions (Table 5).

After the step changes, the distribution of mean monthly streamflow within a water-year has changed across all drainage divisions. Distribution of mean monthly streamflow at four selected gauging stations from four drainage divisions are shown in Fig.11. In northern part of Australia, the increase in streamflow is well-distributed over most of the months. However, in south-west Queensland and southern part of Australia, there seems to be a phase shift as well.

Table 5. Annual and seasonal shifts in different drainage divisions using Pettitt test at $p < 0.10$

Drainage division	Drainage division (no. of stations)	Stations showing shifts				
		Water-year +/-	Autumn +/-	Spring +/-	Summer +/-	Winter +/-
I	North East Coast (66)	0/10	0/3	4/14	0/5	2/21
II	South East Coast (138)	0/83	0/69	3/72	0/56	0/58
III	Tasmania (25)	0/9	0/15	0/0	0/7	0/9
IV	Murray-Darling Basin (133)	0/96	0/81	0/81	1/41	0/98
V	South Australian Gulf (8)	0/5	0/5	0/3	1/5	0/5
VI	South West Coast (50)	0/32	4/27	0/20	5/21	0/34
VII	Pilbara-Gascoyne (10)	2/1	0/1	0/1	2/0	0/3
VIII	Tanami-Timor Sea Coast (21)	13/0	2/0	11/21	13/0	12/0
IX	Carpentaria Coast (10)	1/0	2/0	0/2	2/0	2/0
X	Lake Eyre Basin (4)	0/1	0/1	0/1	0/1	0/2
XI	North Western Plateau (2)	0/0	0/0	0/0	0/0	0/0
XII	South Western Plateau (0)	--	--	--	--	--
Total (467)		16/237	8/202	21/198	24/136	16/230

+ Number of stations showing increasing shifts

- Number of stations showing decreasing shifts

Entries in bold indicate results that are field significant at $p < 0.10$.

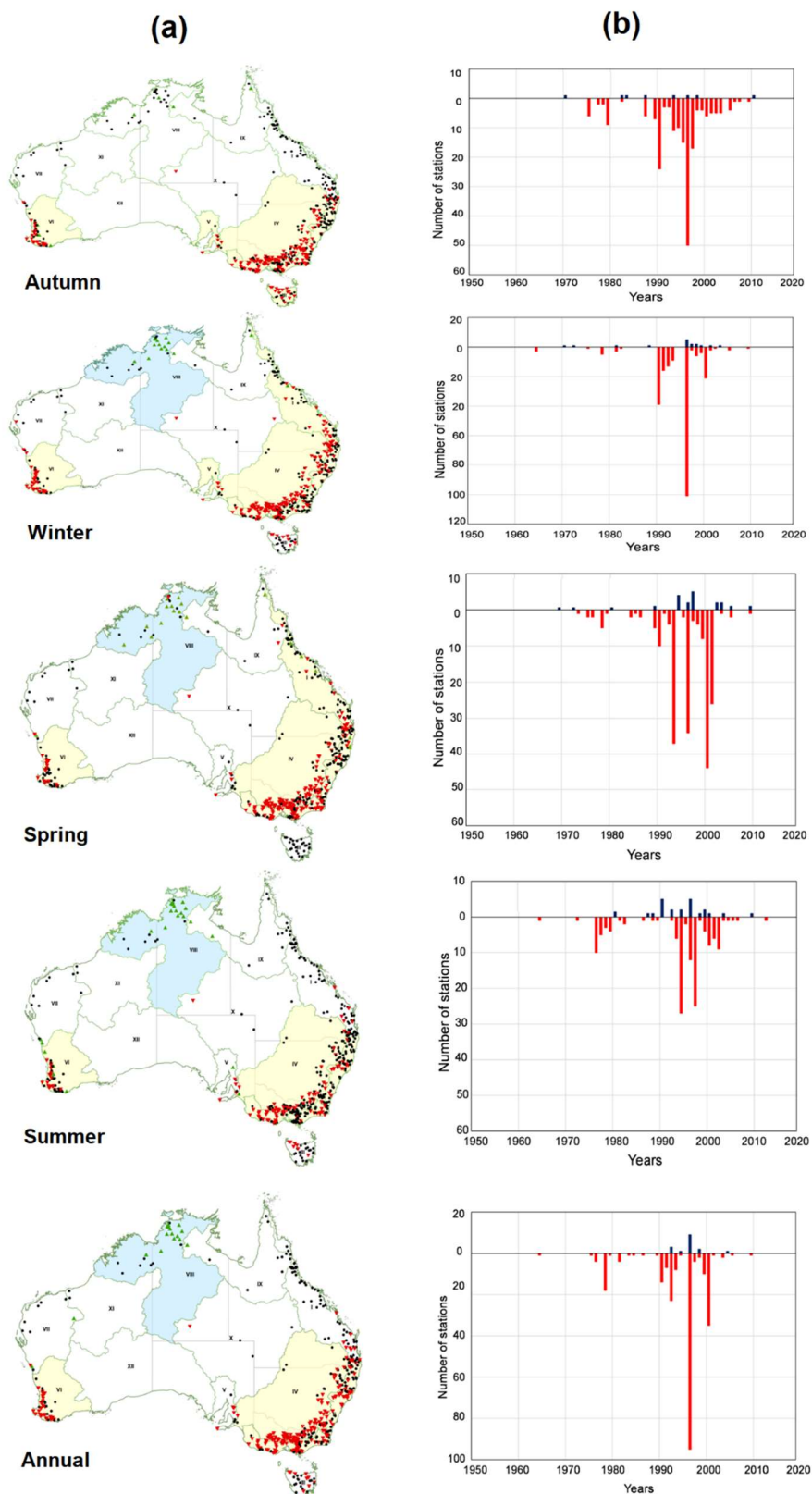


Figure 9: (a) Map showing stations with step changes in flow across each season and water year (at significance level $p < 0.1$), upward pointing green triangles and downward pointing red triangles represent upward and downward step changes, respectively, while black dots refer to sites without significant shifts.

Drainage divisions with positive and negative shifts with field significance at $p < 0.1$ are coloured blue and yellow, respectively. and (b) Number of stations with significant step changes in flows ($p < 0.1$) across each season and water years.

615

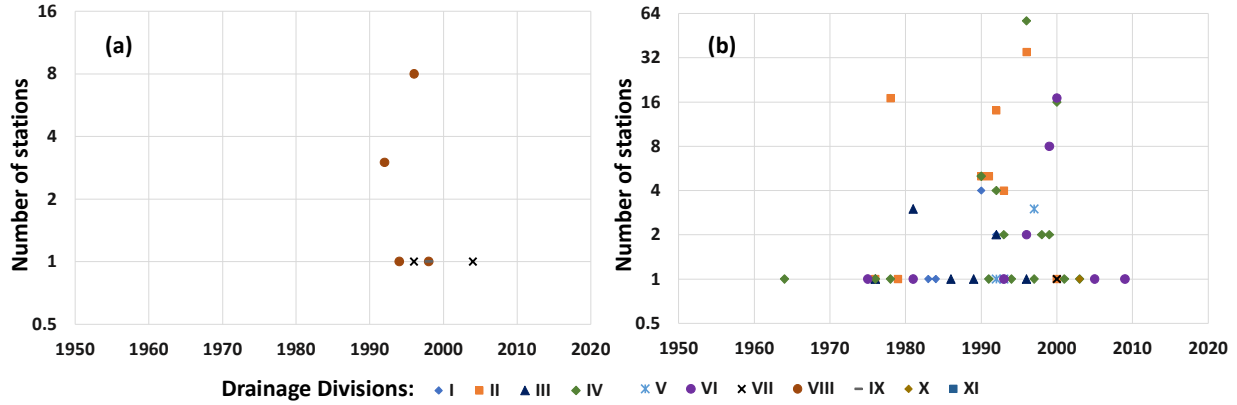


Figure 10: Timing of, and number of stations with step changes for different drainage divisions with (a) increasing and (b) decreasing changes in the water year.

620

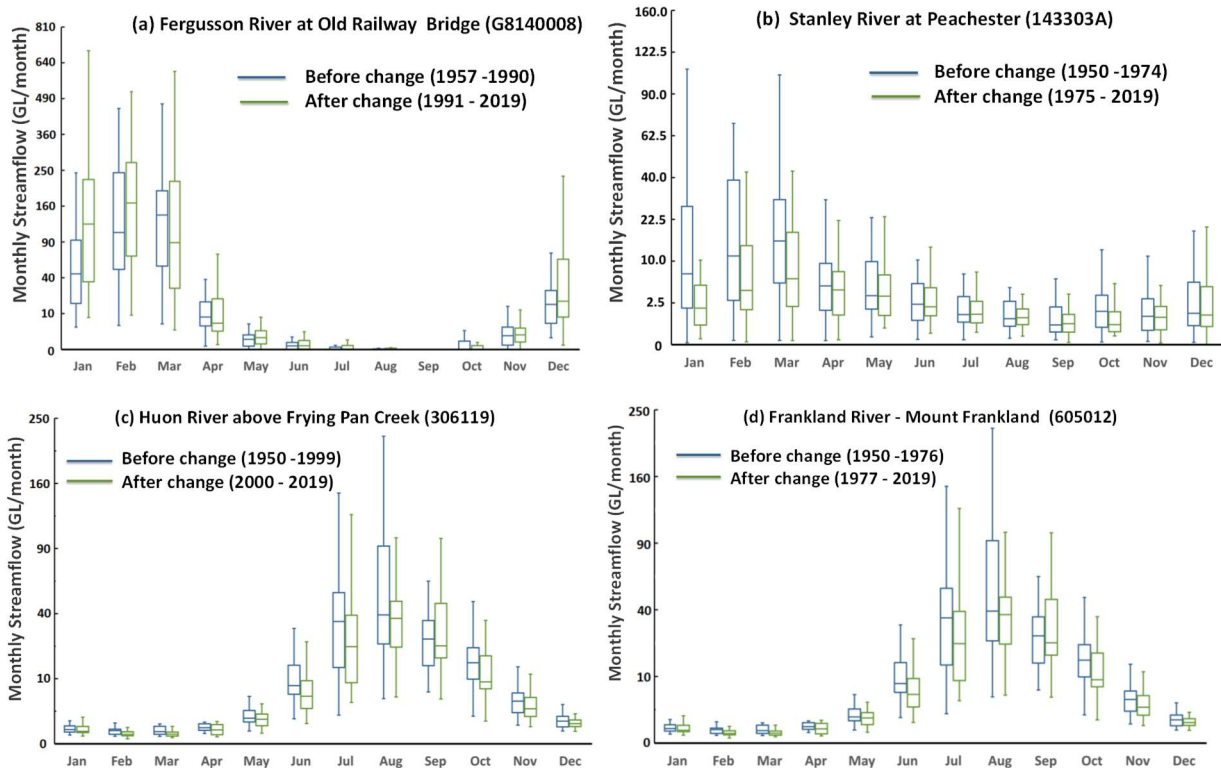


Figure 11: Distribution of mean monthly streamflow before and after step changes at four selected gauging stations representative of (a) Tanami-Timor Sea Coast (VIII), (b) North East Coast (I), (c) Tasmania (III) and (d) South West Coast (VI). See Fig. 1 for locations.

625

4.3 Trend summary of regional significance – drainage divisions

Table 6 summarises field or regional significance at drainage division-scale of monotonic trends and step changes within each drainage division for water year and each of the four seasons. The Murray Darling Basin (IV), South East Coast (I) and South West Coast (VI) divisions experienced decreasing trends for water year, and for all 630 seasons across all statistical tests. Similarly decreasing trends were also evident in the North East Coast (I), Tasmania (III) and South Australian Gulf (V) divisions with the exception of only a few statistical tests (Fig. 7, Fig. 9). In the North East Coast (I) division, only the MK3 test detected no significant annual trends. In the Tasmania (III) division, no step changes (PT) or monotonic trends (Mk4) were detected for spring and summer, respectively. In northern Australia, Tanami- Timor Sea Coast is the only division where most of the statistical 635 tests show increasing trends for water years and for all seasons (Table 6). At annual scales, MK3bs, Mk4 and PT tests showed significant increasing trend. With the exception of autumn, MK3 and PT tests detected increasing monotonic trends for the other three seasons. There were no noticeable patterns in divisions in central Australia, including North Western Plateau (XI) and Lake Eyre Basin (X) divisions. Trends in the Carpentaria Coast (IX) were varied, and only summer saw a significant decreasing trend in flows (MK3). The lack of streamflow 640 observations and relatively low number of stations, or length of records, or number of non-zero flow days in these central Australian divisions may play a role in detecting the trend.

642

643 Table 6 Summary of field significance across different drainage divisions - water year and four seasons

Drainage Division		Water Year				Autumn				Winter				Spring				Summer			
No.	Name	MK3	MK3bs	Mk4	PT	MK3	MK3bs	Mk4	PT	MK3	MK3bs	Mk4	PT	MK3	MK3bs	Mk4	PT	MK3	MK3bs	Mk4	PT
I	North East Coast									✓	✓	✓	✓	✓	✓	✓	✓	✓	✓	✓	✓
II	South East Coast	✓	✓	✓	✓	✓	✓	✓	✓	✓	✓	✓	✓	✓	✓	✓	✓	✓	✓	✓	✓
III	Tasmania	✓	✓	✓		✓	✓	✓		✓	✓	✓			✓	✓		✓	✓	✓	✓
IV	Murray-Darling Basin	✓	✓	✓	✓	✓	✓	✓	✓	✓	✓	✓	✓	✓	✓	✓	✓	✓	✓	✓	✓
V	South Australian Gulf	✓	✓	✓		✓	✓	✓		✓	✓	✓	✓	✓	✓			✓	✓	✓	✓
VI	South West Coast	✓	✓	✓	✓	✓	✓	✓	✓	✓	✓	✓	✓		✓	✓	✓	✓	✓	✓	✓
VII	Pilbara-Gascoyne	✓					✓				✓										
VIII	Tanami-Timor Sea Coast	✓	✓	✓	✓					✓	✓	✓	✓				✓	✓	✓	✓	✓
IX	Carpentaria Coast																				
X	Lake Eyre Basin																				
XI	North Western Plateau																				
XII	South Western Plateau	--	--	--	--	--	--	--	--	--	--	--	--	--	--	--	--	--	--	--	--

644 MK3, MK3bs, MK4 correspond to MK tests

645 PT corresponds to Pettitt Test

646 Entries in bold and non-bold indicate positive upward and negative downward trends, respectively at p < 0.10.

647

5 Discussion

5.1 Data quality and gap-filling

650 To maintain the quality of streamflow data, only gauging stations with less than 25% of flow volume above the recorded maximum gauged discharge and less than 10% of infilled flow volume were included in this study and Hydrologic Reference Stations. A quantitative evaluation of the accuracy of gap-filling procedure showed that gap-filling by interpolation or simple rainfall-runoff modelling is most accurate and effective if the missing record is less than 10% (Zhang and Post, 2018), which was followed in this study. However, when the percentage of 655 gap-filled data represent relatively high end of the flow volume, the uncertainty becomes higher. McMahon and Peel (2019) analysed uncertainties associated with streamflow by considering the gauged and extended range of the stage–discharge relationship from 622 rating curves for 171 of the HRS gauging stations. They found that estimated flow volumes beyond the gauged range of the rating curve occurred in many of these gauging stations and caused measurement uncertainty. As our analysis is limited to seasonal and annual totals, implications of the 660 estimated volumes beyond the gauged range may be minimal.

5.1 Comparison of different tests

665 The MK3 and MK4 tests show there are strong autocorrelations or short-term persistence (STP) and significant long-term persistence (LTP) respectively in Australian streamflow in most drainage divisions (Table 3, Figs. 6). About 85% of stations had data with significant autocorrelation structure (Table 3), and about 40% of these had more than lag-1 autocorrelation (Fig. 3). As such, the MK2 test (Kumar et al., 2009, Su et al., 2018) was not 670 considered in the analysis because it considers only the lag-1 autocorrelation structure. Around 30% of stations had significant LTP only (Table 3). Therefore, two variations of MK3 which considers the total autocorrelation structure (STP) and MK4 which considers LTP behaviour were used in the analysis. Our calculated trends are strongly affected by STP and LTP factors. For water years, there was a clear reduction in number of stations with significant streamflow trends when the full autocorrelation structure (MK3) and LTP behaviour (MK4) were considered in the analysis: from 263 stations with MK1 to 226 with MK3 and 210 with MK4. A similar reduction was observed for most of the seasons (Table 4). Around half of stations with STP and only about 12% of stations with LTP had significant trends for water year as well for all four seasons. The application of these different MK 675 tests helped to differentiate trends that exist under the assumption of serial independence and short and long-term persistence.

680 The Pettitt test showed 54% of stations experienced an abrupt shift in streamflows across water year. Most of these step changes (51%) were decreases and were observed in more stations than for monotonic decreasing trends (38%). Most of the increasing step changes took place in spring (Sep-Nov) and summer (Dec-Feb), whereas most of the decreasing step changes occurred in winter (Jun-Aug). 1970 to 1999 had the largest number of step changes for water year flows. The greatest number of stations (21%) with a decreasing step change was in 1996, whereas most of increasing shifts (2%) occurred in 1996. Seasonally, a greater number of stations with significant decreasing step changes in flow occurred in winter (Fig. 9b-10).

5.3 Attribution of trends

685 For annual time scales, monotonic trends and step changes were similar in direction across the country, however slight variation in direction was observed between seasons and different river basins. These are consistent with previous findings for Australian streamflows (Zhang et al, 2016) and other studies despite having larger number of gauge locations in all drainage divisions except South West Plateau, different analyses methods, length and coverage period of data (Durrant and Byleveld, 2009; Petrone et al., 2010; Tran and Ng, 2009). These findings
690 are consistent with observed changes in rainfall in different parts of Australia (CSIRO and BOM, 2020) where i) Northern Australia has become wetter, particularly in the northwest, with rainfall generally above average in the dry seasons; ii) Australia's climate has warmed on average by about 1.5°C since national records began in 1910, leading to an increase in frequency of extreme heat events and in the length of the fire season, across large parts of the country since the 1950s, especially in southern Australia; iii) For April to October rainfall, there has been
695 a decline of around 16% in the southwest of Australia since 1970 and a decline of around 12% in the southeast of Australia since the late 1990s; iv) Rainfall and streamflow have increased across parts of northern Australia since the 1970s (State of the Climate 2020). In general, observed patterns of rainfall change across the country are expected to continue (CSIRO and BOM, 2020). Research has revealed the association of historical rainfall and soil moisture changes with observed streamflow across different drainage divisions of Australia (Wasko et al.,
700 2021; Wasko and Nathan, 2019). Data from these national network of hydrologic reference stations will be useful for examining and detecting these associations.

Monotonic changes in streamflow generally may occur in response to long-term changes in the flow generation processes including increases or decreases in rainfall, evapotranspiration, temperature, humidity and changes in vegetation dynamics. Note that the catchments considered here are unimpaired, so the impact of anthropogenic
705 activities are not significant. For some of the locations, the decreasing step changes coincide with the Millennium Drought between 1997 to 2009, some catchments underwent changes a few years before that period (Fig. 10). Streamflow deficits in the Murray-Darling Basin were very large during the drought, with an estimated return period of 1 in 1500 years (Gergis et al., 2012), which may be one of the reasons for the largest proportion of stations (96 out of 133) depicting step changes. Sudden and abrupt changes including step changes in streamflow
710 generation process happen due to changes in thresholds which is most prominent when the filling season begins – autumn (Mar-Jun) in south west of Australia (Silberstein et al., 2012) including Tasmania (Fig 9, Table 5). Also evident in phase shift of streamflow distribution in south-west of Western Australia (Fig. 11d), due to reduction in rainfall and lateral shift within the year (Silberstein et al., 2012). Reduction in winter rainfall, increase in temperature and extreme rainfall are projected to continue in the future due to climate change (CSIRO and BOM,
715 2020). Climate change could make extreme events more often – increasing streamflow trend for the wet season, decreasing trend for the dry season and no trend for the annual basis. Increasing atmospheric CO₂ concentration may reduce evapotranspiration rates, which could lead to increased streamflow in certain climatic and geomorphic settings, and this may offset increased evaporation rates due to global warming (Krakauer and Fung, 2008). Recent studies covering south-east of Western Australia suggest the increase in evapotranspiration per unit of rainfall
720 play an important role in streamflow reduction (Fowler et al., in review; Peterson et al., 2021). Questions still remain around how these changes in driving climate forces will interact with each other, and with vegetation, to guide the types and rates of change in streamflow trend.

5.4 Management and further research

The frequency and magnitude of extreme rainfall events have increased across Australia (Sharma et al., 2018) and further investigation is required to understand how this translates to maximum flow and flood extremes in different parts of the country. Changes in the frequency and duration of low flows are also of interest to water managers, particularly in maintaining environmental water flow requirements. Questions remain in relation to phase shifts of streamflow generation within the year (Fig. 11), in particular southern part of Australia. Are they related to rainfall distribution alone, or are there other contributing factors, such as changes in temperature or secondary changes in vegetation dynamics? The influence of step changes on gradual trends was not considered in this study. Further investigation to identify the conditions and processes that result in these step changes would be of great value. Research into these questions is important to guide better management of water resources, infrastructure development and environmental water allocations. The statistical analysis undertaken in this study depends on the length of the time series available, which varies from one station to the next (Fig. 1). In future analyses, streamflow data obtained before the 1950s should be considered for identifying decadal persistence, variability and trends. Better understanding of the nature of trends and step changes in seasonal streamflow can support better regional water management to regulate the flows and maintain adequate levels in reservoirs during dry and wet periods.

6 Summary and Conclusions

Trends in annual and seasonal streamflow over Australia at 467 high quality gauging stations listed in Bureau of Meteorology's [Hydrologic Reference Stations](#) were analysed and presented. Length of the daily streamflow data record ranged from a minimum of 30 years to a maximum of 69 years. Monotonic trend analyses were performed using three different forms of Mann Kendall tests (Variance Correction Approach – MK3, Block Bootstrap Approach – MK3bs and Long-Term Persistence – Mk4). Identification and detection of step changes for seasonal and annual streamflow were accomplished by using nonparametric Pettitt test. Regional significance at different drainage division scale of these changes was analysed and synthesised by using Walker test.

Monotonic decreasing trends in annual and seasonal streamflow at most of the gauging stations were detected in the Murray-Darling River basin and other drainage divisions in New South Wales, Victoria and Tasmania. Similar results were observed in the south-west of Western Australia, South Australia and in north-east Queensland. Decreasing trends in annual totals and in totals for all four seasons were also regionally significant at the drainage division scale. Only the Tanami-Timor Sea Coast drainage division in northern Australia showed increasing trends and step changes in annual and seasonal streamflow, and these were regionally significant. There were no significant spatial and temporal patterns observed in central and mid-west Australia. One possibility for this is the sparse density of streamflow stations and length of data available for analysis.

In general, step changes were similar to the direction of monotonic trends across Australia. Only a handful of stations in northern Australia showed significant step change increases in streamflow. At regional scales, that increasing trend was statistically significant at only the Tanami-Timor Sea Coast drainage division. Across southern Australia, most step changes occurred during 1970-90s, majority of them being in 1990s, before the onset of millennium drought in 1997. Most of the step changes occurred just at the start of winter when the rainy season begins.

760 Further investigation and research would assist to understand the processes that govern the detected changes in flow generation, catchment memory and its interaction with rainfall change, increase in temperature and vegetation growth and evapotranspiration.

7 Acknowledgements

Streamflow data was initially provided by national, State and Territory water agencies across Australia. The 765 Hydrologic Reference Stations website was developed in consultation with The University of Melbourne, CSIRO Land and Water, Department of Climate Change and Energy Efficiency (DCCE) and approximately 70 other stakeholders. We thank Emeritus Professor Tom A. McMahon for his ongoing contribution to the HRS technical review. We express our sincere thanks to the editor, Dr Julien Lerat, Dr Margot Turner, the Bureau of 770 Meteorology's internal reviewers for their careful review and valuable comments and suggestions on the submitted version of this paper. We also thank the three reviewers, whose comments and suggestions greatly improved this paper.

Author Contributions

775 Amirthanathan, G.E. undertook data curation, formal analyses, investigation, methodology, validation, visualisation and writing. Bari, M.A contributed to conceptualisation, investigation, methodology, project administration, resources, supervision, validation and writing. Woldemeskel, F. contributed to data curation, formal analyses, investigation, methodology, validation and visualisation. Feikema, P.M provided project administration, resource allocation, supervision, validation, manuscript review and editing.

780

References

Abdul Aziz, O. I. and Burn, D. H.: Trends and variability in the hydrological regime of the Mackenzie River Basin, *J. Hydrol.*, doi:10.1016/j.jhydrol.2005.06.039, 2006.

785 Akpoti, K., Antwi, E. O. and Kabo-bah, A. T.: Impacts of rainfall variability, land use and land cover change on stream flow of the Black Volta basin, West Africa, *Hydrology*, doi:10.3390/hydrology3030026, 2016.

Alfieri, L., Lorini, V., Hirpa, F. A., Harrigan, S., Zsoter, E., Prudhomme, C. and Salamon, P.: A global streamflow reanalysis for 1980–2018, *J. Hydrol. X*, doi:10.1016/j.hydroa.2019.100049, 2020.

Asadieh, B., Krakauer, N. Y. and Fekete, B. M.: Historical trends in mean and extreme runoff and streamflow based on 790 observations and climate models, *Water (Switzerland)*, doi:10.3390/w8050189, 2016.

Bawden, A. J., Burn, D. H. and Prowse, T. D.: Recent changes in patterns of western Canadian river flow and association with Climatic drivers, *Hydrol. Res.*, doi:10.2166/nh.2014.032, 2015.

Birsan, M. V., Molnar, P., Burlando, P. and Pfaundler, M.: Streamflow trends in Switzerland, *J. Hydrol.*, doi:10.1016/j.jhydrol.2005.06.008, 2005.

795 Bradford, R. B. and Marsh, T. J.: Defining a network of benchmark catchments for the UK, *Proc. Inst. Civ. Eng. Water Marit. Eng.*, doi:10.1680/wame.2003.156.2.109, 2003.

Brimley, B., Cantin, J., Harvey, D., Kowalchuk, M., Marsh, P., Ouarda, T. and Yuzyk, T.: Establishment of the reference hydrometric basin network (RHBN) for Canada., 1999.

Burn, D. H., Whitfield, P. H. and Sharif, M.: Identification of changes in floods and flood regimes in Canada using a peaks 800 over threshold approach, *Hydrol. Process.*, doi:10.1002/hyp.10861, 2016.

BoM (Bureau of Meteorology), CSIRO, 2018. State of the Climate 2018. The third report on Australia's climate by BOM and CSIRO. <http://www.bom.gov.au/state-of-the-climate/>

BoM (Bureau of Meteorology), 2018. Water in Australia 2016-2017, Commonwealth of Australia. Accessed at: <http://www.bom.gov.au/water/waterinaustralia/files/Water-in-Australia-2016-17.pdf>.

805 BoM (Bureau of Meteorology), 2021. Water Dictionary: Water Information: Bureau of Meteorology. Retrieved 7 May 2021, from <http://www.bom.gov.au/water/awid/index.shtml>

BoM (Bureau of Meteorology), 2022. Average annual, seasonal and monthly rainfall, Commonwealth of Australia. Accessed at: http://www.bom.gov.au/jsp/ncc/climate_averages/rainfall/index.jsp

810 Chiew, F. H. S. and McMahon, T. A.: Detection of trend or change in annual flow of Australian rivers, *Int. J. Climatol.*, doi:10.1002/joc.3370130605, 1993.

Coxon, G., Addor, N., Bloomfield, J. P., Freer, J., Fry, M., Hannaford, J., Howden, N. J. K., Lane, R., Lewis, M., Robinson, E. L., Wagener, T. and Woods, R.: CAMELS-GB: hydrometeorological time series and landscape attributes for 671 catchments in Great Britain, *Earth Syst. Sci. Data*, doi:10.5194/essd-12-2459-2020, 2020.

815 Van Dijk, A. I. J. M., Beck, H. E., Crosbie, R. S., De Jeu, R. A. M., Liu, Y. Y., Podger, G. M., Timbal, B. and Viney, N. R.: The Millennium Drought in southeast Australia (2001-2009): Natural and human causes and implications for water resources, ecosystems, economy, and society, *Water Resour. Res.*, doi:10.1002/wrcr.20123, 2013.

Diop, L., Yaseen, Z. M., Bodian, A., Djaman, K. and Brown, L.: Trend analysis of streamflow with different time scales: a case study of the upper Senegal River, *ISH J. Hydraul. Eng.*, doi:10.1080/09715010.2017.1333045, 2018.

820 Dixon, H., Lawler, D. M. and Shamseldin, A. Y.: Streamflow trends in western Britain, *Geophys. Res. Lett.*, doi:10.1029/2006GL027325, 2006.

Do, H. X., Westra, S. and Leonard, M.: A global-scale investigation of trends in annual maximum streamflow, *J. Hydrol.*, doi:10.1016/j.jhydrol.2017.06.015, 2017.

Durrant, J. and Byleveld, S.: Streamflow trends in south-west Western Australia., 2009.

825 Falcone, J. A., Carlisle, D. M., Wolock, D. M. and Meador, M. R.: GAGES: A stream gage database for evaluating natural and altered flow conditions in the conterminous United States, *Ecology*, doi:10.1890/09-0889.1, 2010.

Ficklin, D. L., Abatzoglou, J. T., Robeson, S. M., Null, S. E. and Knouft, J. H.: Natural and managed watersheds show similar responses to recent climate change, *Proc. Natl. Acad. Sci. U. S. A.*, doi:10.1073/pnas.1801026115, 2018.

830 Fiddes, S. and Timbal, B.: Assessment and reconstruction of catchment streamflow trends and variability in response to rainfall across Victoria, Australia, *Clim. Res.*, doi:10.3354/cr01355, 2016.

Fowler, K., Peel, M., Saft, M., Peterson, T., Western, A., Band, L., Petheram, C., Dharmadi, S., Tan, K. S., Zhang, L., Lane, P., Kiem, A., Marshall, L., Griebel, A., Medlyn, B., Ryu, D., Bonotto, G., Wasko, C., Ukkola, A., Stephens, C., Frost, A., Weligamage, H., Saco, P., Zheng, H., Chiew, F., Daly, E., Walker, G., Vervoort, R. W., Hughes, J., Trotter, L., Neal, B., Cartwright, I., and Nathan, R.: Explaining changes in rainfall-runoff relationships during and after Australia's Millennium Drought: a community perspective, *Hydrol. Earth Syst. Sci. Discuss. [preprint]*, <https://doi.org/10.5194/hess-2022-147>, in review, 2022.

Gergis, J., Gallant, A. J. E., Braganza, K., Karoly, D. J., Allen, K., Cullen, L., D'Arrigo, R., Goodwin, I., Grierson, P. and McGregor, S.: On the long-term context of the 1997-2009 “Big Dry” in South-Eastern Australia: Insights from a 206-year multi-proxy rainfall reconstruction, *Clim. Change*, doi:10.1007/s10584-011-0263-x, 2012.

840 Gudmundsson, L., Leonard, M., Do, H. X., Westra, S. and Seneviratne, S. I.: Observed Trends in Global Indicators of Mean and Extreme Streamflow, *Geophys. Res. Lett.*, doi:10.1029/2018GL079725, 2019.

Hamed, K. H. and Ramachandra Rao, A.: A modified Mann-Kendall trend test for autocorrelated data, *J. Hydrol.*, doi:10.1016/S0022-1694(97)00125-X, 1998.

Helsel, D. R., Hirsch, R. M., Ryberg, K. R., Archfield, S. A. and Gilroy, E. J.: Statistical methods in water resources: U.S. 845 Geological Survey Techniques and Methods, book 4, chapter A3, B. 4, *Hydrol. Anal. Interpret.*, 2020.

Herawati, H., Suripin and Suharyanto: Impact of climate change on streamflow in the tropical Lowland of Kapuas River, West Borneo, Indonesia, in *Procedia Engineering*, 2015.

Hodgkins, G. A., Dudley, R. W., Russell, A. M. and Lafontaine, J. H.: Comparing trends in modeled and observed streamflows at minimally altered basins in the United States, *Water (Switzerland)*, doi:10.3390/W12061728, 2020.

850 Holper, P.: Australian rainfall: past, present and future., 2011.

Ishak, E. H., Rahman, A., Westra, S., Sharma, A. and Kuczera, G.: Preliminary analysis of trends in Australian flood data, in World Environmental and Water Resources Congress 2010: Challenges of Change - Proceedings of the World Environmental and Water Resources Congress 2010., 2010.

Kendall, M.: *Rank Correlation Methods*, 4th ed., Charles Griffin, London, UK., 1975.

855 Khaliq, M. N., Ouarda, T. B. M. J. and Gachon, P.: Identification of temporal trends in annual and seasonal low flows occurring in Canadian rivers: The effect of short- and long-term persistence, *J. Hydrol.*, doi:10.1016/j.jhydrol.2009.02.045, 2009.

Korhonen, J. and Kuusisto, E.: Long-term changes in the discharge regime in Finland, *Hydrol. Res.*, doi:10.2166/nh.2010.112, 2010.

Koutsoyiannis, D.: Climate change, the Hurst phenomenon, and hydrological statistics, *Hydrol. Sci. J.*, 860 doi:10.1623/hysj.48.1.3.43481, 2003.

Krakauer, N. Y., and I. Fung (2008), Mapping and attribution of change in streamflow in the coterminous United States, *Hydrol. Earth Syst. Sci.*, 12(4), 1111–1120, doi:10.5194/hess-12-1111-2008.

Kumar, S., Merwade, V., Kam, J. and Thurner, K.: Streamflow trends in Indiana: Effects of long term persistence, precipitation and subsurface drains, *J. Hydrol.*, doi:10.1016/j.jhydrol.2009.06.012, 2009.

865 Kundzewicz, Z. and Robson, A.: Detecting Trend and Other Changes in Hydrological Data. Word Climate Program-Data and Monitoring, Geneva., 2000.

Li, L., Zou, Y., Li, Y., Lin, H., Liu, D. L., Wang, B., Yao, N. and Song, S.: Trends, change points and spatial variability in extreme precipitation events from 1961 to 2017 in China, *Hydrol. Res.*, doi:10.2166/nh.2020.095, 2020.

Lins, H. F.: USGS Hydro-Climatic Data Network 2009 (HCDN-2009), U.S. Geol. Surv., 2012.

870 Lins, H. F. and Slack, J. R.: Streamflow trends in the United States, *Geophys. Res. Lett.*, doi:10.1029/1998GL900291, 1999.

Mallakpour, I., Villarini, G., 2016. A simulation study to examine the sensitivity of the Pettitt test to detect abrupt changes in mean. *Hydrol. Sci. J.* 61, 245–254. <https://doi.org/10.1080/02626667.2015.1008482>.

Mann, H. B.: Non-Parametric Test Against Trend, *Econometrica*, 1945.

McMahon, T. A. and Peel, M. C.: Uncertainty in stage–discharge rating curves: application to Australian Hydrologic Reference 875 Stations data, *Hydrol. Sci. J.*, doi:10.1080/02626667.2019.1577555, 2019.

Milly, P. C. D., Dunne, K. A. and Vecchia, A. V.: Global pattern of trends in streamflow and water availability in a changing climate, *Nature*, doi:10.1038/nature04312, 2005.

Nicholls, N., Drosdowsky, W. and Lavery, B.: Australian rainfall variability and change, *Weather*, doi:10.1002/j.1477-8696.1997.tb06274.x, 1997.

880 O’Neil, H. C. L., Prowse, T. D., Bonsal, B. R. and Dibike, Y. B.: Spatial and temporal characteristics in streamflow-related hydroclimatic variables over western Canada. Part 1: 1950-2010, *Hydrol. Res.*, doi:10.2166/nh.2016.057, 2017.

Önöz, B. and Bayazit, M.: The power of statistical tests for trend detection, *Turkish J. Eng. Environ. Sci.*, doi:10.3906/sag-1205-120, 2003.

Pan, Z., Ruan, X., Qian, M., Hua, J., Shan, N. and Xu, J.: Spatio-temporal variability of streamflow in the Huaihe River Basin, 885 China: Climate variability or human activities?, *Hydrol. Res.*, doi:10.2166/nh.2017.155, 2018.

Perrin, C., Michel, C. and Andréassian, V.: Improvement of a parsimonious model for streamflow simulation, *J. Hydrol.*, doi:10.1016/S0022-1694(03)00225-7, 2003.

Petrone, K. C., Hughes, J. D., Van Niel, T. G. and Silberstein, R. P.: Streamflow decline in southwestern Australia, 1950-2008, *Geophys. Res. Lett.*, doi:10.1029/2010GL043102, 2010.

890 Pettitt, A. N.: A Non-Parametric Approach to the Change-Point Problem, *Appl. Stat.*, doi:10.2307/2346729, 1979.

Poff, N. L. R., Olden, J. D., Pepin, D. M. and Bledsoe, B. P.: Placing global stream flow variability in geographic and

geomorphic contexts, *River Res. Appl.*, doi:10.1002/rra.902, 2006.

Politis, D. N.: The Impact of Bootstrap Methods on Time Series Analysis, *Stat. Sci.*, doi:10.1214/ss/1063994977, 2003.

Rao, A., Hamed, K. and Chen, H.: Nonstationarities in hydrologic and environmental time series, Springer., 2003.

895 Rice, J. S., Emanuel, R. E., Vose, J. M. and Nelson, S. A. C.: Continental U.S. streamflow trends from 1940 to 2009 and their relationships with watershed spatial characteristics, *Water Resour. Res.*, doi:10.1002/2014WR016367, 2015.

Sagarika, S., Kalra, A. and Ahmad, S.: Evaluating the effect of persistence on long-term trends and analyzing step changes in streamflows of the continental United States, *J. Hydrol.*, doi:10.1016/j.jhydrol.2014.05.002, 2014.

900 Sen, P. K.: Estimates of the Regression Coefficient Based on Kendall's Tau, *J. Am. Stat. Assoc.*, doi:10.1080/01621459.1968.10480934, 1968.

Sharma, A., Wasko, C. and Lettenmaier, D. P.: If Precipitation Extremes Are Increasing, Why Aren't Floods?, *Water Resour. Res.*, doi:10.1029/2018WR023749, 2018.

905 Silberstein, R. P., Aryal, S. K., Durrant, J., Pearcey, M., Braccia, M., Charles, S. P., Boniecka, L., Hodgson, G. A., Bari, M. A., Viney, N. R. and McFarlane, D. J.: Climate change and runoff in south-western Australia, *J. Hydrol.*, doi:10.1016/j.jhydrol.2012.02.009, 2012.

Stern, H., De Hoedt, G. and Ernst, J.: Objective classification of Australian climates, *Aust. Meteorol. Mag.*, 2000.

von Storch, H.: Misuses of statistical analysis in climate research. In: von Storch, H., Navarra, A. (Eds.), *Analysis of Climate Variability: Applications of Statistical Techniques*, in Springer-Verlag, Berlin., 1995.

910 Svensson, C., Kundzewicz, Z. W. and Maurer, T.: Trend detection in river flow series: 2. Flood and low-flow index series, *Hydrol. Sci. J.*, doi:10.1623/hysj.2005.50.5.811, 2005.

Theil, H.: A rank-invariant method of linear and polynomial regression analysis, Part I, *Proc. R. Netherlands Acad. Sci.*, 1950.

Tran, H. and Ng, A.: Statistical trend analysis of river streamflows in Victoria, in H2O09: 32nd Hydrology and Water Resources Symposium, pp. 1019–1027, Engineers Australia. [online] Available from: <https://search.informit.org/doi/10.3316/informit.757692124391804>, 2009.

915 Villarini, G., Serinaldi, F., Smith, J. A. and Krajewski, W. F.: On the stationarity of annual flood peaks in the continental United States during the 20th century, *Water Resour. Res.*, doi:10.1029/2008WR007645, 2009.

Wasko, C. and Sharma, A.: Global assessment of flood and storm extremes with increased temperatures, *Sci. Rep.*, doi:10.1038/s41598-017-08481-1, 2017.

Wasko, C., Nathan, R., 2019. Influence of changes in rainfall and soil moisture on trends in flooding. *J. Hydrol.* 575, 432–441.

920 <https://doi.org/10.1016/j.jhydrol.2019.05.054>.

Wasko, C., Nathan, R. and Peel, M. C.: Trends in Global Flood and Streamflow Timing Based on Local Water Year, *Water Resour. Res.*, doi:10.1029/2020WR027233, 2020.

Wasko, C., Shao, Y., Vogel, E., Wilson, L., Wang, Q.J., Frost, A., Donnelly, C., 2021. Understanding trends in hydrologic extremes across Australia. *J. Hydrol.* 593, 125877. <https://doi.org/10.1016/j.jhydrol.2020.125877>.

925 Whitfield, P. H., Burn, D. H., Hannaford, J., Higgins, H., Hodgkins, G. A., Marsh, T. and Looser, U.: Reference hydrologic networks I. The status and potential future directions of national reference hydrologic networks for detecting trends, *Hydrol. Sci. J.*, doi:10.1080/02626667.2012.728706, 2012.

Wilks, D. S.: On “field significance” and the false discovery rate, *J. Appl. Meteorol. Climatol.*, doi:10.1175/JAM2404.1, 2006.

Williams, A. N.: A new population curve for prehistoric Australia, *Proc. R. Soc. B Biol. Sci.*, doi:10.1098/rspb.2013.0486, 930 2013.

Yue, S., Pilon, P., Phinney, B. and Cavadias, G.: The influence of autocorrelation on the ability to detect trend in hydrological series, *Hydrol. Process.*, doi:10.1002/hyp.1095, 2002.

935 Zhang, X. S., Amirthanathan, G. E., Bari, M. A., Laugesen, R. M., Shin, D., Kent, D. M., MacDonald, A. M., Turner, M. E. and Tuteja, N. K.: How streamflow has changed across Australia since the 1950s: Evidence from the network of hydrologic reference stations, *Hydrol. Earth Syst. Sci.*, doi:10.5194/hess-20-3947-2016, 2016.

Zhang, Y. and Post, D.: How good are hydrological models for gap-filling streamflow data?, *Hydrol. Earth Syst. Sci.*, doi:10.5194/hess-22-4593-2018, 2018.

Zhang, Y., Viney, N., Frost, A., Oke, A., Brooks, M., Chen, Y. and Cambell, N.: Collation of Australian modeller’s streamflow dataset for 780 unregulated Australian catchments., 2013.

940